Botanical Journal of the Linnean Society, 2024, **XX**, 1–30
https://doi.org/10.1093/botlinnean/boae029
Advance access publication 28 May 2024
Original Article

OXFORD

Original Article

Floral structure, histochemistry, and volatile compounds in *Bulbophyllum* species of the '*Cirrhopetalum* alliance' (Orchidaceae)

Kevin L. Davies[1] Małgorzata Stpiczyńska[2], Richard A. Ludlow[3], Louise Wheaton[3], Danilo Aros[3,4], Frank Hailer[3], Carsten T. Müller[3] and Hilary J. Rogers[3,*]

[1]School of Earth and Environmental Sciences, Cardiff University, Main Building, Park Place, Cardiff CF10 3AT, UK
[2]Faculty of Biology, Botanic Garden, University of Warsaw, Al. Ujazdowskie 4, 00-478 Warsaw, Poland
[3]School of Biosciences, Cardiff University, Sir Martin Evans Building, Museum Avenue, Cardiff, CF10 3AX, UK
[4]Faculty of Agricultural Sciences, University of Chile, Santiago, Chile

[*]Corresponding author. School of Biosciences, Cardiff University, Sir Martin Evans Building, Museum Avenue, Cardiff, CF10 3AX, UK. E-mail: rogershj@cardiff.ac.uk

ABSTRACT

Bulbophyllum is the most species-rich orchid genus. Recent molecular data groups certain of its species into a monophyletic '*Cirrhopetalum* alliance'. Within this alliance are a monophyletic section *Cirrhopetaloides* and a non-monophyletic section *Cirrhopetalum*. Floral morphology and scent are partially conserved phylogenetically compared to the molecular data. Here, floral morphology, histochemistry, anatomy, and floral volatile organic compounds (VOCs) of selected *Bulbophyllum* species are analysed to assess whether there are structural or chemical differences that support separation into the two sections, to update available VOC data from this genus, and to consider evolutionary adaptations in the '*Cirrhopetalum* alliance'. We found that '*Cirrhopetalum* alliance' flowers differ from some sections of *Bulbophyllum* in the structure of cells lining the longitudinal groove on the labellum or lip and report, for the first time in *Bulbophyllum*, a type of atypical oleiferous trichome probably involved in VOC production. We show a clear difference in floral VOC profiles between *B. bicolor* (sect. *Cirrhopetaloides*) and four other *Bulbophyllum* species, three previously assigned to sect. *Cirrhopetalum*, but VOC profiles do not support separation into the two sections. The lack of congruence between already established molecular phylogeny, floral anatomy, and VOC data suggests that VOC differences are due to recently and independently evolved pollinator specificity. We therefore show that there is no clear separation of these sections based on floral anatomy, histochemistry, or VOC profiles.

Keywords: *Bulbophyllum*; DNA analysis; fragrance; labellum; micromorphology; Orchidaceae; sect. *Cirrhopetaloides*; sect. *Cirrhopetalum*; ultrastructure; VOC analysis

INTRODUCTION

Bulbophyllum Thouars is the largest orchid genus comprising an estimated 2200 species. Distributed throughout the tropics from Africa, Asia, Australia, New Zealand, and the tropical Pacific islands as far east as Tahiti to the Neotropics, the main centres of distribution are Madagascar (200 species) and New Guinea (600 species) (Pridgeon *et al.* 2014). The genus represents an excellent model system to study the evolution of plant–pollinator interactions and to understand the drivers of rapid plant diversification (Hu *et al.* 2020).

The most comprehensive recent taxonomic study of *Bulbophyllum* is presented in a chapter by de Camargo Smidt, Fischer, Gravendeel, and Vermeulen in *Genera Orchidacearum Vol. 6* (Pridgeon *et al.* 2014), which lists 68, 12, and six sections of *Bulbophyllum* occurring in Asia, continental Africa, and the Neotropics, respectively. These authors distinguish between sections *Cirrhopetalum* (Lindl.) Rchb.f. (nine species) and *Cirrhopetaloides* Garay, Hamer & Siegerist (19 species) (see Supporting Information, Table S1). Many Asian species currently assigned to these two sections, including all those studied here (Table 1), were previously united in the former genus *Cirrhopetalum* Lindl. (Garay *et al.* 1994), as they share a range of vegetative and floral morphological features. Many of the 10 species investigated here are currently accepted as belonging to

Received 11 January 2024; revised 4 April 2024; accepted 27 April 2024

Table 1. Species of *Bulbophyllum* and type of investigation undertaken.

Species	Source and accession number	Determined by./ confirmed by	Section with references	Gross morphology/ micromorphology	Anatomy	Histo-chemistry	VOCs	DNA
B. bicolor Lindl.	KLD 201711	Conf. KLD	Sect. *Cirrhopetaloides* Garay, Hamer & Siegerist (Hu *et al.* 2020)	+/+	+	+	+	+
B. bicolor Lindl.	KLD 201809	Conf. KLD	Sect. *Cirrhopetaloides* Garay, Hamer & Siegerist (Hu *et al.* 2020)	+/−				
B. bicolor Lindl.	KLD 201810	Conf. KLD	Sect. *Cirrhopetaloides* Garay, Hamer & Siegerist (Hu *et al.* 2020)	+/−				
B. eberhardtii (Gagnep.) Seidenf.	KLD 201208	Det. JJV	Sect. *Cirrhopetalum* (Lindl.) Rchb.f. (IOSPE and Retrieved 2022)	+/+	+	+		
B. fascinator (Rolfe) Rolfe var. *semi-album*	KLD 201820	Conf. KLD	Sect. *Cirrhopetalum* (Lindl.) Rchb.f. (Vermeulen 1991) Sect. *Cirrhopetaloides* Garay, Hamer & Siegerist. (Vermeulen O'Byrne and Lamb 2015, Hu *et al.* 2020)	+/+	+	+		
B. longibrachiatum Z.H. Tsi	MP1	Det. JJV	Probably Sect. *Cirrhopetalum* (Lindl.) Rchb.f. (IOSPE and Retrieved 2022)	+/+	+	+		
B. longiflorum Thouars	KLD 201322	Conf. KLD	Sect. *Cirrhopetalum* (Lindl.) Rchb.f. (Vermeulen 1991, Vermeulen and O'Byrne 2011, Pridgeon *et al.* 2014, Vermeulen, O'Byrne and Lamb 2015, Hu *et al.* 2020)	+/+	+	+	+	+
B. longiflorum Thouars	KLD 201414	Det. JJV	Sect. *Cirrhopetalum* (Lindl.) Rchb.f. (Vermeulen 1991, Vermeulen and O'Byrne 2011, Pridgeon *et al.* 2014, Vermeulen O'Byrne and Lamb 2015, Hu *et al.* 2020)	+/+	+	+		
B. longiflorum Thouars	KLD 201811	Conf. KLD	Sect. *Cirrhopetalum* (Lindl.) Rchb.f. (Vermeulen 1991, Vermeulen and O'Byrne 2011, Pridgeon *et al.* 2014, Vermeulen, O'Byrne and Lamb 2015, Hu *et al.* 2020)	+/−				
B. longiflorum Thouars	MP6	Conf. KLD	Sect. *Cirrhopetalum* (Lindl.) Rchb.f. (Vermeulen 1991, Vermeulen and O'Byrne 2011, Pridgeon *et al.* 2014, Vermeulen, O'Byrne and Lamb 2015, Hu *et al.* 2020)	+/−			+	+
B. longiflorum Thouars	KLD 201802 Yellow form	Conf. KLD	Sect. *Cirrhopetalum* (Lindl.) Rchb.f. (Vermeulen 1991, Vermeulen and O'Byrne 2011, Pridgeon *et al.* 2014, Vermeulen, O'Byrne and Lamb 2015, Hu *et al.* 2020)	+/+	+	+		
B. ornatissimum (Rchb.f.) J.J. Sm.	KLD 201821	Conf. KLD	Probably Sect. *Cirrhopetaloides* Garay, Hamer & Siegerist (IOSPE and Retrieved 2022)	+/+	+	+		
B. pecten-veneris (Gagnep.) Seidenf.	KLD 201318	Det. JJV	Sect. *Cirrhopetalum* (Lindl.) Rchb.f. (Hu *et al.* 2020)	+/+	+	+	+	
B. pecten-veneris (Gagnep.) Seidenf.	MP2	Conf. KLD	Sect. *Cirrhopetalum* (Lindl.) Rchb.f. (Hu *et al.* 2020)	+/−			+	+
B. picturatum (Lodd.) Rchb.f.	KLD 201714	Det. KLD	Sect. *Cirrhopetalum* (Lindl.) Rchb.f. (Hu *et al.* 2020)	+/+	+	+		

Table 1. Continued

Species	Source and accession number	Determined by./ confirmed by	Section with references	Gross morphology/ micromorphology	Anatomy	Histo-chemistry	VOCs	DNA
B. picturatum (Lodd.) Rchb.f.	BN	Conf. KLD	Sect. *Cirrhopetalum* (Lindl.) Rchb.f. (Hu *et al.* 2020)	+/–			+	+
B. rothschildianum (O'Brien) J.J. Sm.	KLD 201712 Red form	Conf. KLD	Sect. *Cirrhopetaloides* Garay, Hamer & Siegerist (Hu *et al.* 2020)	+/+	+	+	+	+
B. rothschildianum (O'Brien) J.J. Sm.	KLD 201713 Brown form	Conf. KLD	Sect. *Cirrhopetaloides* Garay, Hamer & Siegerist (Hu *et al.* 2020)	+/+	+	+	+	
B. rothschildianum (O'Brien) J.J. Sm.	MP3	Conf. KLD	Sect. *Cirrhopetaloides* Garay, Hamer & Siegerist (Hu *et al.* 2020)	+/–			+	+
B. rothschildianum (O'Brien) J.J. Sm.	MP4	Conf. KLD	Sect. *Cirrhopetaloides* Garay, Hamer & Siegerist (Hu *et al.* 2020)	+/–			+	
B. sanguineopunctatum Seidenf. & A.D. Kerr	MP5	Det. JJV	Sect. *Cirrhopetaloides* Garay, Hamer & Siegerist (Hu *et al.* 2020)	+/+	+	+		

Accessions prefixed KLD were obtained from the first author's collection, those labelled MP and BN from Malcolm Perry (Frampton Cottrell, UK) and Burnham Nurseries Ltd (Newton Abbot, UK), respectively. Identities were determined (Det.) or confirmed (Conf.) by J.J. Vermeulen (JJV) or the first author (KLD).

section *Cirrhopetalum* (Lindl.) Rchb.f., with as many as five species possibly belonging to sect. *Cirrhopetaloides* Garay, Hamer & Siegerist. However, owing to the paucity of published information, which species ought to be assigned to each of these two sections is unclear. Hu *et al.* (2020) grouped them all into the '*Cirrhopetalum* alliance', adding that 'the homogeneous morphology of vegetative characters and homoplastic flowers, even between distantly related *Cirrhopetalum* species, renders sectional taxonomy problematic, even for specialists'. Similarly, although recent phylogenetic analyses have classed *Bulbophyllum* as monophyletic (Chase *et al.* 2015), the large number of species contained therein complicate the inference of precise infrageneric relationships. Two successive classifications have been suggested (Garay *et al.* 1994, Vermeulen *et al.* 2014), but further work (Wang *et al.* 2017) based on a larger number of markers yielded contrasting results. More recently, a phylogeny constructed for the '*Cirrhopetalum* alliance' based on four DNA markers, onto which floral characters were mapped (Hu *et al.* 2020), strongly supports this alliance as a monophyletic group, and divides it into four major clades and seven subclades. Note that this new phylogeny includes the section *Desmosanthes*, not previously considered part of *Cirrhopetalum* s.l. Attempts have also been made to compare phylogeny from sequence analysis to VOC profiles (Nakahira *et al.* 2018) although, so far, only a limited number of species has been investigated.

The pollination of many *Bulbophyllum* spp. has been well documented. Flowers of *Bulbophyllum* are among the most morphologically diverse of all orchids (Gravendeel *et al.* 2004), and their pollination mechanisms among the most intricate (van der Cingel 2001). *Bulbophyllum* species are entomophilous, and most conform to the fly-pollination syndrome (van der Cingel 2001), being either myophilous or sapromyophilous. Pollinators include Diptera such as fruit flies, Drosophilidae (Ong 2011, Ong *et al.* 2011 and references therein, Ong and Tan 2012); blowflies, Calliphoridae; and flesh flies, Sarcophagidae of both sexes (Ong and Tan 2011, Ong 2012; Stpiczyńska *et al.* 2018a, b); as well as other dipterans, such as Platystomatidae, Milichiidae, Chloropidae, Sciridae, Tachinidae, and Tephritidae (Pridgeon *et al.* 2014); together with Hymenoptera, such as bees, Apidae, and wasps, including stingless bees and ctenuchid wasps (Johansson 1974, cited in Dressler 1990, 1993, van der Cingel 2001), and even some foraging Coleoptera. Pollinator specificity is common (Chen and Gao 2011, Humeau *et al.* 2011), with mimicry perhaps occurring in certain *Bulbophyllum* species (Knerr 1981, Koehler and Davenport 1983, Christensen 1994). Attraction of insect pollinators to the *Bulbophyllum* flower is achieved by a combination of flower colour (usually dull cream or yellow-green to purple-brown and frequently spotted); mobile floral parts, such as hinged labella and appendages; epidermal hairs, papillae and glands; and floral rewards such as oil and nectar, as well as potent floral scents (Silva *et al.* 1999).

Floral-food rewards, however, are relatively uncommon among orchids and of these, nectar is the most common, although oil and resin-like secretions are also frequently present (van der Pijl and Dodson 1969, van der Cingel 2001, Davies and Stpiczyńska 2008 and references therein). Floral-food rewards have only rarely been documented for *Bulbophyllum* (Pohl 1935, Jongejan 1994, van der Cingel 2001), but in the last few years, a number of studies have demonstrated histochemically that the

labella of several African, Asian, and Neotropical representatives of this genus produce lipid- and/or protein-rich, viscid secretions, sometimes together with sugar, whereas others produce a mainly sugar-rich secretion or nectar (Davies and Stpiczyńska 2014, Nunes *et al.* 2014, 2015, 2017a, Stpiczyńska *et al.* 2015, 2018a, Stpiczyńska and Davies 2016, Stpiczyńska *et al* 2018b) which *Drosophila* and *Bactrocera* fruit flies drink from the longitudinal, median labellar groove, or sulcus (Ong 2011, Ong *et al.* 2011 and references therein, Ong and Tan 2012).

Only rarely has the anatomical basis of food rewards and fragrance production been investigated for *Bulbophyllum* (Davies and Stpiczyńska 2014, Nunes *et al.* 2014, Kowalkowska *et al.* 2015, Nunes *et al.* 2015, Stpiczyńska *et al.* 2015, Stpiczyńska and Davies 2016, Kowalkowska *et al.* 2017, Nunes *et al.* 2017a, Stpiczyńska *et al.* 2018a, b). In many families, including Orchidaceae, floral scents are produced in complex secretory, specialized glands called osmophores (Esau 1965, Vogel 1990). It is known that phenylpropanoid compounds present in the fragrance of some *Bulbophyllum* species are used by male flies for boosting their defence system and synthesizing pheromones that attract females (Tan and Nishida 2000, 2005, Tan *et al.* 2002). Difficulties in obtaining volatile organic compound (VOC) profiles from small-flowered *Bulbophyllum* species has led to the use of extraction methods using alcohol (e.g. Tan and Nishida 2000, Katte *et al.* 2020), high pressure Soxhlet extraction using CO_2 followed by microhydrodistillation or solid sample injection (Silva *et al.* 1999). More recently, solid phase microextraction has also been applied (Humeau *et al.* 2011). Similar fragrance compositions are now considered more indicative of shared pollinators than shared phylogeny (e.g. Nunes *et al.* 2017b). Conversely, different ecotypes of the same orchid species offering either nectar or oil as reward have been shown to have similar floral scents, and species of the same genus sharing the same pollinator can have different scents (Powers *et al.* 2020, Castañeda-Zárate *et al.* 2021). Evolutionary changes in VOC profile may occur with a change in pollinators in sexually deceptive orchids (Ayasse *et al.* 2011), but are less well studied in other orchid clades. *Bulbophyllum* floral fragrance composition has revealed distinct VOC abundance patterns correlated with pollinators. Chen *et al.* (2005) listed >60 constituents for the genus, including flavonoids, phenylpropanoids, and stilbenoids (the last typically present in most species), including phenanthrenes, dihydrophenanthrenes (including dimeric forms), and bibenzyls. Of these stilbenoids, five from *Bulbophyllum andersonii* (cited as *Cirrhopetalum andersonii*) were unique to *Bulbophyllum*, including the phenanthrene cirrhopetalin, the dihydrophenanthrene cirrhopetalanthridin, and the bibenzyls cirrhopetalidin, cirrhopetalinin, and cirrhopetalidinin (Majumder and Basak 1990, 1991a, b). However, more recent and more sensitive methods for VOC analysis, such as thermal desorption gas chromatography time-of-flight mass spectrometry, that can discriminate subtle differences in plant VOC profiles (e.g. in peach fruit, Sirangelo *et al.* 2022), have not to our knowledge been applied to *Bulbophyllum* and could provide useful information on VOC profile differences in relation to morphology.

The currently accepted separate grouping of many similar species in either sect. *Cirrhopetalum* (including the sectional type species *B. longiflorum*) or sect. *Cirrhopetaloides*, previously combined in *Cirrhopetalum* Lindl., warrants further investigation. Therefore, the aim of this work was to ascertain whether separation of these species into two sections is justified on the basis of floral anatomy, histochemistry and VOC analyses. A further aim was to provide an updated study of VOCs and micromorphology/anatomy from selected *Bulbophyllum* species of the '*Cirrhopetalum* alliance', in the context of their phylogeny, taxonomy, and possible evolutionary adaptations.

MATERIALS AND METHODS

Plant material

The morphology, micromorphology, anatomy, and histochemistry of 10 greenhouse-grown *Bulbophyllum* species once considered to belong in *Cirrhopetalum* Lindl. and obtained from various sources (Table 1) were investigated. Of these, four, *B. eberhardtii* (Gagnep.) Seidenf., *B. longiflorum* Thouars, *B. pecten-veneris* (Gagnep.) Seidenf., and *B. picturatum* (Lodd.) Rchb.f. have since been assigned to sect. *Cirrhopetalum*, and three, *B. bicolor* Lindl., *B. rothschildianum* (O'Brien) J.J. Sm. and *B. sanguineopunctatum* Seidenf. & A.D. Kerr, are now considered to belong in sect. *Cirrhopetaloides*. Two other species, *B. longibrachiatum* Z.H. Tsi and *B. ornatissimum* (Rchb.f.) J.J. Sm., probably belong in sections *Cirrhopetalum* and *Cirrhopetaloides*, respectively, whereas *B. fascinator* (Rolfe) Rolfe, has, at various times, been assigned to both sections (Table 1). Note that *B. longiflorum* is the type species for sect. *Cirrhopetalum* and occurs both in Asia and continental Africa.

Phylogenetic analysis of DNA from analysed leaf material was employed to confirm the taxonomic identity of five of the species investigated.

Spirit-preserved, voucher material of each accession was deposited at the herbarium of the Royal Botanic Gardens, Kew, UK under the general accession number Davies 2022 1-10. Abbreviations for authors of plant names follow Brummitt and Powell (1992) throughout.

Microscopy and histochemistry

Intact flowers of each species were tested with glucose-sensitive sticks (Diastix, Bayer). Sufficient surface secretion was produced in each case to test directly for glucose without having to collect labellar washings. The flowers were subsequently immersed in histochemical stain solutions, both to detect putative secretory tissues and to ascertain their chemical composition and that of any surface secretion present. These stains included saturated ethanolic Sudan III solution to detect lipids, aqueous 0.05% (w/v) ruthenium red (RR) solution for pectins and mucilage (Jensen 1962), and 0.25% (w/v) Coomassie Brilliant Blue R 250 (CBB) in 7% (v/v) acetic acid (Fisher 1968) for proteins. Stained flowers were examined using a Nikon SMZ1000 stereoscopic microscope. Secretory tissues were subsequently examined using light microscopy or Nomarski differential interference microscopy. Semi-thin sections of material fixed in 2.5% (v/v) glutaraldehyde/4% (v/v) formaldehyde in 0.1 M phosphate buffer pH 7.4 were stained (i) for general histology using a 1:1 mixture of 1% (w/v) aqueous methylene blue: 1% (w/v) aqueous azure II (MB/AII), (ii) insoluble polysaccharides using the periodic acid-Schiff reaction (Jensen 1962), (iii) for lipids with 0.3% (w/v) ethanolic Sudan Black B solution or a saturated

ethanolic solution of Sudan IV, and (iv) for volatile terpenoids with 1% (w/v) aqueous solution of OsO_4 (Stern *et al.* 1986). Fixed, hand-sectioned floral material was also stained with CBB for proteins, IKI (aqueous iodine-potassium iodide solution) for starch, an ethanolic solution of Sudan IV for lipids and RR for mucilage. Micromorphology and ultrastructure of the floral parts were investigated with scanning electron microscopy (SEM) and transmission electron microscopy (TEM), respectively, as described previously (Davies and Stpiczyńska 2014, Stpiczyńska *et al.* 2015, Stpiczyńska and Davies 2016).

Epifluorescence microscopy (FM) of fixed material using a Nikon Eclipse N*i*-U upright microscope equipped with a Prior 200 W lamp (Prior Scientific Instruments Ltd) and UV-2B cube filter 355/50 (330–380 nm excitation filter; a 400 nm (LP) dichroic mirror; and a 435 nm (LP) barrier filter) was undertaken to detect autofluorescence of cell walls, cuticle, and epicuticular waxes. The presence of volatile oils in hand-sectioned material was investigated by staining floral parts with neutral red (NR) and examining them under UV light (Kirk 1970), or with auramine O (Gahan 1984, Ruzin 1999) and examining under blue light using a fluorescein isothiocyanate-Nikon cube filter to investigate the structure of the cuticle.

Micrometry and photomicrography were accomplished using a DS-Fi1 digital camera (Nikon, Japan) and NIS-Elements BR software, and a high-resolution digital camera (CCD MORADA, SiS-Olympus, Germany) for light microscopy and TEM images, respectively.

For SEM, floral parts were dehydrated in acetone and subjected to critical-point drying using liquid CO_2 before being sputter-coated with gold and examined using a LEO 1430VP (Zeiss) or a Hitachi S-4700 (Hitachi, Tokyo, Japan) scanning electron microscope, at accelerating voltages of 30 and 20 kV, respectively.

VOC analysis

VOCs were collected from the headspace of flowers from five species of *Bulbophyllum*: *Bulbophyllum bicolor* Lindl., *B. longiflorum* Thouars, *B. pecten-veneris* (Gagnep.) Seidenf., *B. picturatum* (Lodd.) Rchb.f., and *B. rothschildianum* (O'Brien) J.J. Sm. (Table 1), as previously described (Spadafora *et al.* 2016). Inflorescences of each specimen were placed into a nalophan bag (medium size, Lakeland), and left for 30 min to equilibrate. A total of 2.5 L of headspace was collected onto SafeLok thermal desorption tubes (Tenax TA, Sulficarb, Markes International) using a manual grab pump (Easy-VOC, Markes International). Air samples were also collected as blanks for each sample.

Samples were desorbed from the tubes in a TD100 (Markes International) for 5 min at 120°C followed by 5 min at 280°C with 50 mL/min nitrogen onto the trap at 25°C. The trap was desorbed at 300°C for 3 min with 7 mL/min helium. The compounds were separated in a GC9000 (Agilent) on a 60 m, 0.32 mm ID, 0.5 µm Rtx-5ms capillary column (Restek) with 1.5 mL/min helium at constant flow. The temperature programme started with 2 min at the initial temperature of 40°C followed by a linear gradient of 5°C/min to 280°C and a post run of 5 min at 300°C.

Compounds were detected using a BenchTOFtx time-of-flight mass spectrometer (Markes International) operated at 280°C transfer line temperature and 240°C ion source temperature with 4600 scans/scan-set from *m/z* 35 to 650. A retention index standard (C8—C20, 40 mg/L, Supelco) was analysed under the same conditions after injection of 1 µL of standard directly onto a TD tube.

Data were inspected in Chemstation (Agilent) and analysed in AMDIS v.2.72 (NIST). AMDIS was used to deconvolute traces. A retention indexed mass spectral library was constructed in AMDIS from searches in the NIST mass spectral library. Compounds were included as 'putatively identified' if they showed a match factor > 80% in mass spectrum and matched RI (±20). Components that returned match factors > 80% but no matching RI were included as e.g. 'alkane'. Compounds that recurred at the same RI between samples, consistently showed the same mass spectrum but yielded no library hit were included as 'unknown'. Aligned data were checked for consistency in RI (relative standard deviation < 1%) across samples. Components present in blanks and known contaminants were removed and areas normalized for further analyses. Areas were normalized to the total VOC area for each sample, providing a relative abundance for each VOC in each sample. The square root of the relative abundance was used for further data analysis to reduce the weighting of highly abundant VOCs. Zero values were replaced with an arbitrary value of one-tenth of the minimum value for the whole dataset reflecting the fact that these compounds were below the limit of detection of the mass spectrometer but not necessarily completely absent, which a zero value would incorrectly imply.

Data analysis was conducted using the 'adonis' function in the package 'vegan' (Oksanen *et al.* 2013) and 'CAP-discrim' function in the package 'BiodiversityR' (Kindt and Coe 2005) of R v.3.5.2. These were used to perform permutational multivariate analysis of variance (PERMANOVA) (Anderson and Legendre 1999) and canonical analysis of principal coordinates (CAP) (Anderson and Willis 2003), respectively. Metaboanalyst v.4.0 (Chong *et al.* 2018) was used to perform random forest analysis as a supervised machine-learning algorithm (Pang *et al.* 2020).

DNA extraction, amplification, and sequencing to verify identification of samples

DNA extractions were carried out on samples from the same five species (*Bulbophyllum bicolor*, *B. longiflorum*, *B. pecten-veneris*, *B. picturatum*, and *B. rothschildianum*) used for VOC analyses, using an Extract-N-Amp PCR kit (Sigma-Aldrich). Small portions, maximum 0.5 cm across, were removed from the edges of fresh leaves from each sample, stored at −80°C, and placed in 250 µL PCR tubes containing 40 µL of extraction buffer. Tubes were centrifuged in a Minispin Eppendorf microcentrifuge for 30 s at 13 500 rpm. Each sample was then ground in the extraction buffer using a sterile 200 µL pipette tip. The samples were placed in a Veriti thermal cycler (Applied Biosystems) and heated to 95°C for 10 min. Samples were allowed to cool to room temperature, before 40 µL of dilution buffer was added. Samples were then mixed, centrifuged for 2–5 min to pellet leaf debris, and the resulting lysate was used for subsequent PCR reactions.

PCR primers 390F (5′-CGATCTATTCATTCAATATTTC-3′) and 1326R (5′-TCTAGCACACGAAAGTCGAAGT-3′) (Cuénoud *et al.* 2002) were used to amplify ~900 bp of the *matK* gene, and primers ITS4 (5′–TCCTCCGCTTATTGATATGC) and ITS5 (5′– GGAAGTAAAAGTCGTAACAAGG) (White *et al.* 1990) to amplify ~700 bp of the *ITS* region. PCR reactions

comprised 1.25 µL of DNA extract, 5 µL of 5× green Go Taq flexi buffer (Promega, Madison, WI, USA), 2 µL of 25 mM $MgCl_2$ (Promega, Madison, WI, USA), 1 µL each of the primers (at 9 µM), 0.5 µL of 10 mM dNTPs, 0.125 µL of Go Taq flexi DNA polymerase (Promega, Madison, WI, USA), and 14 µL of sterile water. PCRs were amplified on a Veriti thermal cycler (Applied Biosystems) as follows for *matK* primers: 94°C for 4 min, 35 cycles of 94 °C for 1 min, 48°C for 30 s, and 72°C for 1 min, with a 7 min final extension at 72°C. For *ITS* primers, amplification was 98°C for 5 min, 38 cycles of 98°C for 45 s, 50°C for 45 s, and 72°C for 2 min, with a 10 min final extension at 72°C. PCR success was verified by electrophoresis on agarose gels.

PCR products were purified using a QIA Quick PCR Purification kit (Qiagen, Crawley, UK) according to the manufacturer's instructions and sequenced by Eurofins genomics using both forward and reverse primers. Sequences were deposited in the GenBank database (accession numbers for *matK*: KLD 201711: OM687356; BN: OM687357; MP2: OM687358; KLD 201318: OM687359; KLD 201712: OM687360; MP3: OM687361; KLD 201322: OM687362; accession numbers for *ITS*: OP451904, OP451905, OP451906, OP451907, OP451908).

Phylogenetic trees

Forward and reverse DNA sequences from each sample were aligned using Bioedit software v.4.0.6.2 and aligned using the ClustalW multisequence alignment tool, to produce consensus sequences. Additional sequences were obtained from the Entrez NCBI database for *ITS* [*B. bicolor* (KY022455, KY966430, KY966431, KY966432), *B. picturatum* (EF195939), *B. pecten-veneris* (JN619418, KY966471, KY966470), *B. longiflorum* (EF196024, EF196023) and *B. rothschildianum* (KX455819)], and *matK* [*B. bicolor* (KY966722 and KY966723), *B. pecten-veneris* (KY966761 and KY966762) and *B. rothschildianum* (KX455835)]. *matK* and *ITS* GenBank sequences from *Dendrobium officinale* (MG760737 and MH244306, respectively) were selected as the outgroup. Sequence alignment was performed in Mega software v.7 (Kumar *et al.* 2016) using the Muscle plugin. A phylogenetic tree was produced using the maximum likelihood approach implemented in IQ-Tree2 (Minh *et al.* 2020) on a devoted web server (Trifinopoulos *et al.* 2016), with 5000 ultrafast bootstrap replications (Hoang *et al.* 2018) to determine branch support. The modelfinder approach in IQ-Tree2 was used to determine the best fitting model of sequence evolution, including 'freerate' rate heterogeneity (Kalyaanamoorthy *et al.* 2017).

RESULTS

Floral morphology, micromorphological, anatomical, and histochemical investigations

In the present study, gross morphology, micromorphology, anatomy, ultrastructure, and histochemical investigations of the flowers of *Bulbophyllum eberhardtii* (Fig. 1A), *B. fascinator* var. *semi-album* (Fig. 1B), *B. longibrachiatum* (not shown), *B. longiflorum* (Fig. 1C, D), *B. pecten-veneris* (Fig. 1E), *B. ornatissimum* (Fig. 1F), *B. picturatum* (Fig. 1G), *B. sanguineopunctatum* (not shown), *B. rothschildianum* (Fig. 1H), and *B. bicolor* (Fig. 1I), all members of the '*Cirrhopetalum* alliance', were undertaken.

Characteristic features of these species, as described in the literature and confirmed here, are that they possess subumbellate inflorescences and their flowers have (i) dorsal sepals and petals that frequently bear clavate projections or multicellular, flag-like appendages called paleae, and thus appear fringed (Fig. 1A–H); (ii) significantly elongated lateral sepals that are twisted and connate for at least part of their length, such that their abaxial surfaces are uppermost and initially remain fused to each other to form a shallow longitudinal groove along which the lateral sepals later separate (Fig. 1A–I); and (iii) a mobile or rocking labellum with a relatively deep, median longitudinal groove or sulcus (Fig. 1A–I). Paleae (Fig. 1J), and other epidermal structures, such as fimbriae and laciniae, contain oil droplets, and often occur along the margins of perianth segments. However, a remarkable feature of *B. pecten-veneris*, not previously reported for any other species of *Bulbophyllum* to our knowledge, is the presence of atypical, multiseriate, multicellular trichomes that are distributed along the margins of the dorsal sepal and petals (Fig. 2A–D). These possess a striate cuticle (Fig. 2D) and contain large, intravacuolar lipid droplets (Fig. 2E–G). Sunken trichomes are also present basally on the dorsal sepal and petals of this species. By contrast, the atrichomatous epidermal cells and the ground parenchyma cells of both these organs, contain numerous, very small lipid droplets, greater quantities occurring in the marginal epidermal cells (Fig. 2H). Viscid secretions or silvery secretory residues occur within and along the labellar sulcus, often less copiously on the abaxial surface (now uppermost) of the lateral sepals. In some species, this secretion is so copious that it obfuscates the topography of the labellar epidermis (e.g. *B. eberhardtii*—Fig. 3A). The morphological and anatomical characteristics of each individual species are summarized in Table 2.

Transverse sections through the labellum of all investigated species, as exemplified here by *B. fascinator* var. *semi-album* (Fig. 3B), reveal that the sulcus is lined with cuboidal to rectangular epidermal cells below which occur 1–3 subepidermal layers. The cells of both epidermis and subepidermal layers are secretory and contain varying quantities of lipid droplets of various sizes (e.g. *B. longibrachiatum*—Fig. 3C), which also occur in the marginal epidermal cells and trichomes of the labellum (e.g. *B. longiflorum* and *B. rothschildianum*—Fig. 3D–F). These are also present in the other perianth segments, predominantly in the abaxial epidermal cells of the lateral sepals (e.g. *B. rothschildianum*—Fig. 4A), which are uppermost owing to the twisting of the sepals, but sometimes also in the dorsal sepal and petals (e.g. *B. rothschildianum*). The size variation in these droplets indicates that some may represent droplets of volatile oils. The latter are usually much smaller and much more numerous than typical lipid droplets and tend to occur mainly in marginal epidermal cells and trichomes, with the larger lipid droplets perhaps acting as precursors in the formation of volatile oil droplets. The surface secretion of perianth segments, such as occurs on the lateral sepals, also contains lipid, whereas that of the labellum sometimes also contains protein. The occurrence of intracellular lipid droplets and the distribution of surface secretion are summarized in Tables 2 and 3.

No typical, specialized osmophores (relatively complex, multicellular, fragrance-producing epidermal structures or glands) are present (*B. picturatum*, *B. rothschildianum*, and *B. bicolor*). Instead, volatile oil droplets are produced by relatively

Figure 1. Inflorescences and gross floral morphology of representatives of the '*Cirrhopetalum* alliance'. A, Habit of flowers of *Bulbophyllum eberhardtii* (KLD 201208) arranged on a subumbellate inflorescence. B, Lateral view of flower of *B. fascinator* var. *semi-album* (KLD 201820) showing floral parts. Note the verrucose, fused lateral sepals, distinctly grooved labellum and purple paleae on the dorsal sepal and petals. C, D, Subumbellate inflorescences of *B. longiflorum* showing variation in flower colour. C and D represent inflorescences and flowers of accessions KLD 201414 and KLD 201802, respectively. E, The inflorescence of *B. pecten-veneris* (KLD 201318) is more compact than those of the other

unspecialized epidermal cells of the perianth segments that selectively stain with NR, Sudan stains, and osmium tetroxide. These cells occur on the lateral sepals (Fig. 4A), and to a lesser degree, on the dorsal sepal projections or appendages, and occasionally on petals (Fig. 2H). Most, however, occur on the labellum (Figs 3C–F, 4C), and regardless of organ, usually have a marginal distribution, again perhaps facilitating the diffusion of fragrance. Unlike the palisade-like secretory labellar epidermal cells found in many species of *Bulbophyllum* studied to date (e.g. Davies and Stpiczyńska 2014, Stpiczyńska *et al.* 2015, 2018a, b, Stpiczyńska and Davies 2016), those of the '*Cirrhopetalum* alliance' are cuboidal or only slightly elongate, with the exception of *B. longibrachiatum* (Fig. 3C), where somewhat more palisade-like cells sometimes occur. The epidermis and subepidermal tissue enclose the central ground parenchyma which contains collateral vascular bundles (Fig. 3B) and idioblasts with raphides. The cuticle overlying the epidermal secretory cells lining the sulcus often becomes distended and blistered as secretion accumulates between it and the outer tangential cell wall of the epidermis before becoming deposited on the surface of the labellum (Figs 3A, 4B, C). Cuticular blistering and surface material were also observed for the lateral sepals of some species (Table 3).

The epidermal cells lining the median longitudinal groove of the labellum, together with subepidermal tissue have an organelle complement typical of lipid-secretory cells (Fig. 4E, F), generally with abundant arrays of endoplasmic reticulum [mainly smooth endoplasmic reticulum (SER)], mitochondria, secretory vesicles, multivesicular bodies, dictyosomes (Golgi bodies), and plastids (mainly chromoplasts) with typical plastoglobuli and starch grains. Lipid droplets (precursors of fragrance production) are also abundant in both the labellum and labellar trichomes (Fig. 4D, E). The irregular or undulating outline of the plasmalemma (Fig. 4E, F) in some species is indicative of granulocrine secretion. Whereas the mitochondria contain abundant cristae (Fig. 4E), typical of highly metabolic secretory cells, the plastids often contain well-developed internal membranes, starch grains, and typical plastoglobuli. Highly organized arrays of rough endoplasmic reticulum and SER are often present (Fig. 4E, F). SER is usually the more predominant, often displaying distended cisternae, and is associated with small secretory vesicles that gather in the peripheral cytoplasm and become associated with the plasmalemma, or occur in the periplasmic space (Fig. 4F). Lipid droplets are also frequent both here and in subepidermal cells, and are probably derived from plastoglobuli, whereas dictyosomes (Golgi bodies) are often associated with both SER and secretory vesicles, together forming the Golgi–endoplasmic reticulum–lysosome (GERL) complex (Fig. 4E). The close juxtaposition of the various organelles forming the GERL complex indicates that they are together involved in lipid biosynthesis. Multivesicular bodies are also frequent in epidermal and subepidermal cells. Furthermore, the enormous numbers of free ribosomes present are typical of highly metabolic protein-producing cells. TEM investigations of the epidermal and subepidermal cells of the labellum of *B. rothschildianum* revealed that the cell walls are irregularly thickened or have undulating contours (Fig. 4F), thereby increasing the surface area for secretion. Numerous primary pit fields with abundant plasmodesmata present in several species are indicative of efficient symplastic transport, and in *B. rothschildianum*, secretory vesicles, as well as gathering in the parietal cytoplasm of the labellum and becoming associated with the plasmalemma, also gather in labellar trichomes, as also occurs in *B. bicolor* (Fig. 4D). The thick cuticle overlying the labellar trichomes of both these species contains numerous micro-channels (Fig. 4D) that are probably involved in the passage of secretion onto the labellar surface.

Analysis of VOC profiles for five *Bulbophyllum* species

A phylogenetic analysis based on two markers (*matK* and *ITS*) was used to putatively verify species identity of the samples used for VOC analysis (Fig. S1 in the Supporting Information). Maximum likelihood phylogenetic analysis grouped most samples with available *ITS* sequences by species (including available sequence data from GenBank), and was in agreement with the established phylogeny of Hu *et al.* (2020). However, the newly obtained *B. rothschildianum* sequences were divergent from the database sequence. The *matK* based phylogeny was broadly in agreement, but with overall lower resolution and bootstrap support values.

A total of 44 VOCs were detected across all *Bulbophyllum* species sampled: *B. bicolor*, *B. longiflorum*, *B. pecten-veneris*, *B. picturatum*, and *B. rothschildianum* (Tables S2 and S3 in the Supporting Information). The profile across all the species comprised alkanes (20), terpenes (six), alcohols (five), esters (four), ketones (three), aldehydes and aromatic compounds (two of each), and free acids (one). The highest number of VOCs was detected in *B. rothschildianum* (15) followed by *B. picturatum* and *B. pecten-veneris* (10 in each), *B. bicolor* (seven), and *B. longiflorum* (five). 1-Butanol was the VOC present in most species (only absent from *B. picturatum*), and no individual VOC was present in all species tested. In *B. picturatum* and *B. pecten-veneris*, the VOC family with the highest relative abundance was the alkanes, while in *B. rothschildianum* and *B. bicolor,* terpenes dominated the profile, and in *B. longiflorum* alcohols were most abundant. However, there were few statistically significant differences in the relative abundance of VOC families among the different species (ANOVA, $P < 0.05$): the only differences were a greater relative abundance of alkanes in *B. rothschildianum*

species investigated and the delicate flowers inserted almost vertically on it. F, Subumbellate inflorescence and flowers of *B. ornatissimum* (KLD 201821) showing stages in the separation of the lateral sepals. G, Detail of flowers of *B. picturatum* (KLD 201714) showing grooved mobile labellum and terminal, clavate projection to the dorsal sepal. H, Flowers of the brown form (KLD 201713) of *B. rothschildianum.* The tongue-like labellum is distinctly grooved and mobile, the dorsal sepal and petals bear elongate paleae, and the twisted lateral sepals are clearly seen to be fused along their margins. I, Flowers of *B. bicolor* (KLD 201711). Note the mobile, grooved lip and that the lateral sepals are no longer fused together. J, Whole mount of individual paleae of petal of *B. fascinator* var. *semi-album* (KLD 201820), as viewed using Nomarski differential interference microscopy. Scale bars: A–F, I, 10 mm; G, H, 5 mm; J, 100 μm. KEY: ac = anther cap; c = column; ds = dorsal sepal; la = labellum; ls = lateral sepal; pe = petal; s = stelidium.

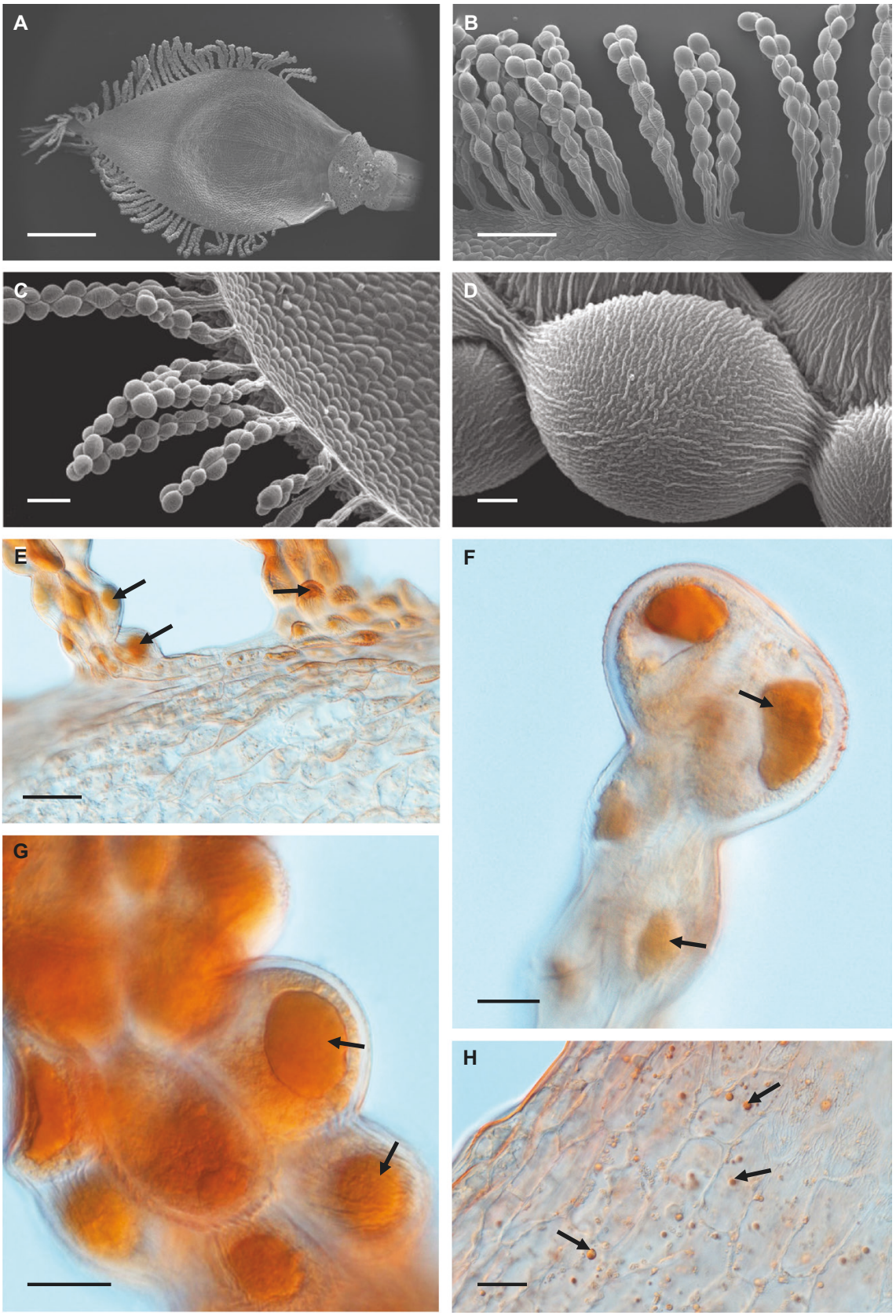

Figure 2. Structure and histochemistry of floral parts of *Bulbophyllum pecten-veneris* (KLD 201318). A, SEM of dorsal sepal showing terminal tuft of appendages and marginal, multiseriate, multicellular trichomes. B, C, Detail of marginal, multiseriate trichomes of dorsal sepal and petal, respectively. D, Detail of striate cuticle of marginal trichome of dorsal sepal. E, Margin of petal with bases of multiseriate, oleiferous trichomes treated with Sudan IV. Note that this reagent selectively stains intravacuolar lipid bodies in the trichomes (arrows). F, G, Detail of apex and stalk of multiseriate, oleiferous trichome, respectively, treated with Sudan IV. Note the large intravacuolar lipid bodies (arrows) and minute lipid droplets on the external wall surface of the terminal cells. H, Detail of petal surface, treated with Sudan IV, showing numerous, small lipid bodies (arrows). Scale bars: A, 1 mm; B, 200 μm; C, 100 μm; D, 10 μm; E, 50 μm; F, G, H, 20 μm.

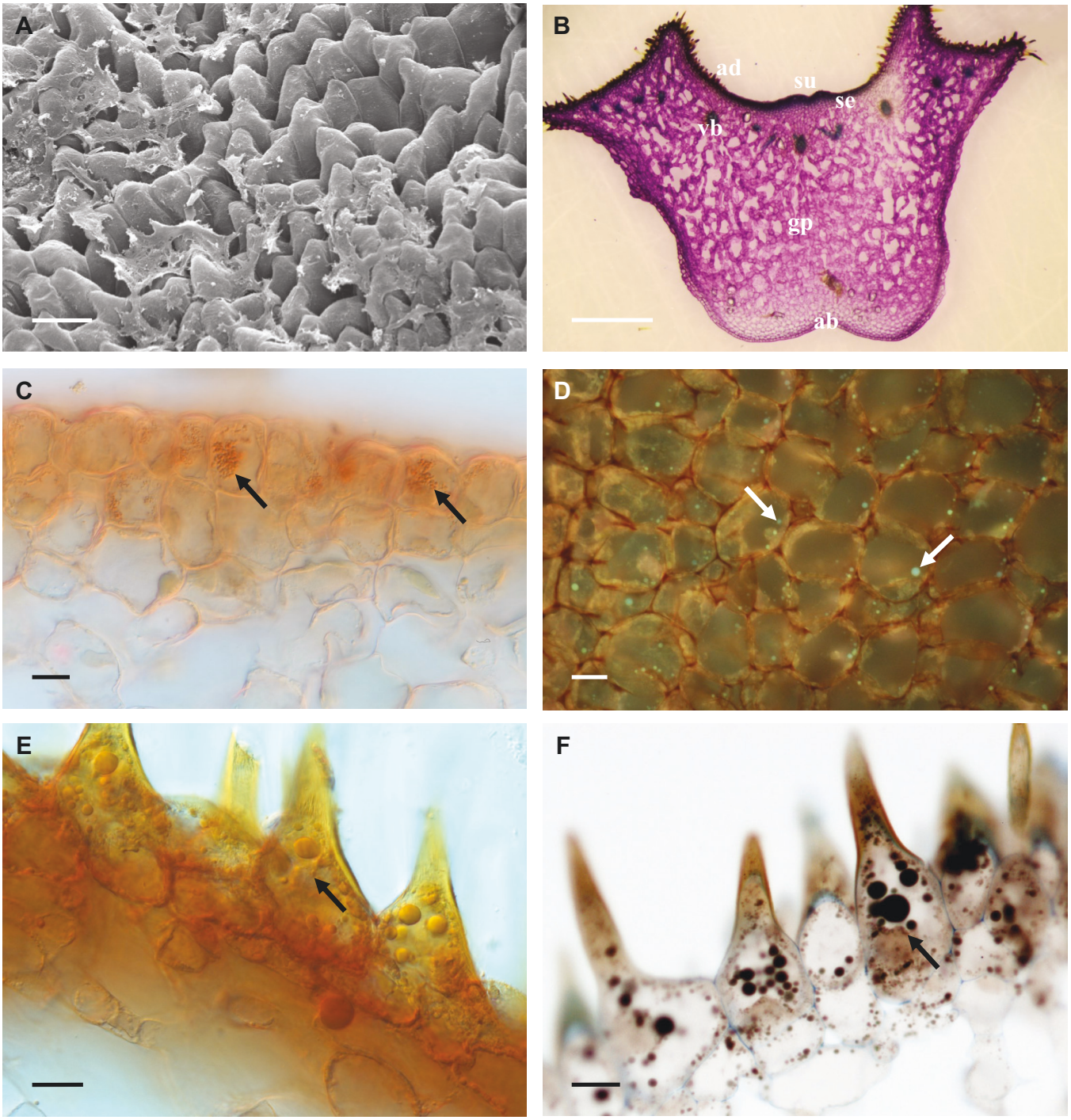

Figure 3. Floral anatomy and histochemistry of *Bulbophyllum eberhardtii*, *B. fascinator* var. *semi-album*, *B. longibrachiatum*, *B. longiflorum*, and *B. rothschildianum*. A, Detail of papillose adaxial surface of labellum of *Bulbophyllum eberhardtii* (KLD 201208), as seen using SEM, obfuscated by residues of secreted material. B, Transverse section of labellum of *B. fascinator* var. *semi-album* (KLD 201820) stained with MB/AII showing typical labellar anatomy, with hirsute adaxial epidermal cells, subepidermal parenchyma, and ground parenchyma in which occur vascular bundles and often, idioblasts containing bundles of raphides. The adaxial, median longitudinal groove or sulcus is flanked by keels and lined with secretory epidermal cells. C, Labellar epidermal cells of *B. longibrachiatum* (MP1) containing numerous droplets of volatile compounds (arrows), stained with Sudan IV. D, Adaxial labellar epidermis of *B. longiflorum* (KLD 201414) stained with NR and viewed under UV, showing distribution of lipid droplets (arrows). E, F, Marginal trichomes of labellum of *B. rothschildianum* (KLD 201712) stained with Sudan IV (E), and both TBO and osmium tetroxide (F) for droplets of volatile compounds (arrows). Scale bars: A, C–F, 20 μm; B, 1 mm. KEY: ab = abaxial epidermis; ad = adaxial epidermis; gp = ground parenchyma; se = subepidermis; su = sulcus; vb = vascular bundle.

compared to *B. bicolor*, and of aromatic compounds in *B. bicolor* and *B. picturatum* compared to *B. rothschildianum*.

Using all 44 VOCs, profiles showed a significantly different pattern of relative abundance of the VOCs across the species (PERMANOVA, $P < 0.05$, $R^2 = 0.011$). Using linear discriminant plots from canonical analysis of principal coordinates (CAP), VOCs discriminated *B. bicolor* from all other species, and also discriminated between *B. longiflorum* and *B. picturatum*,

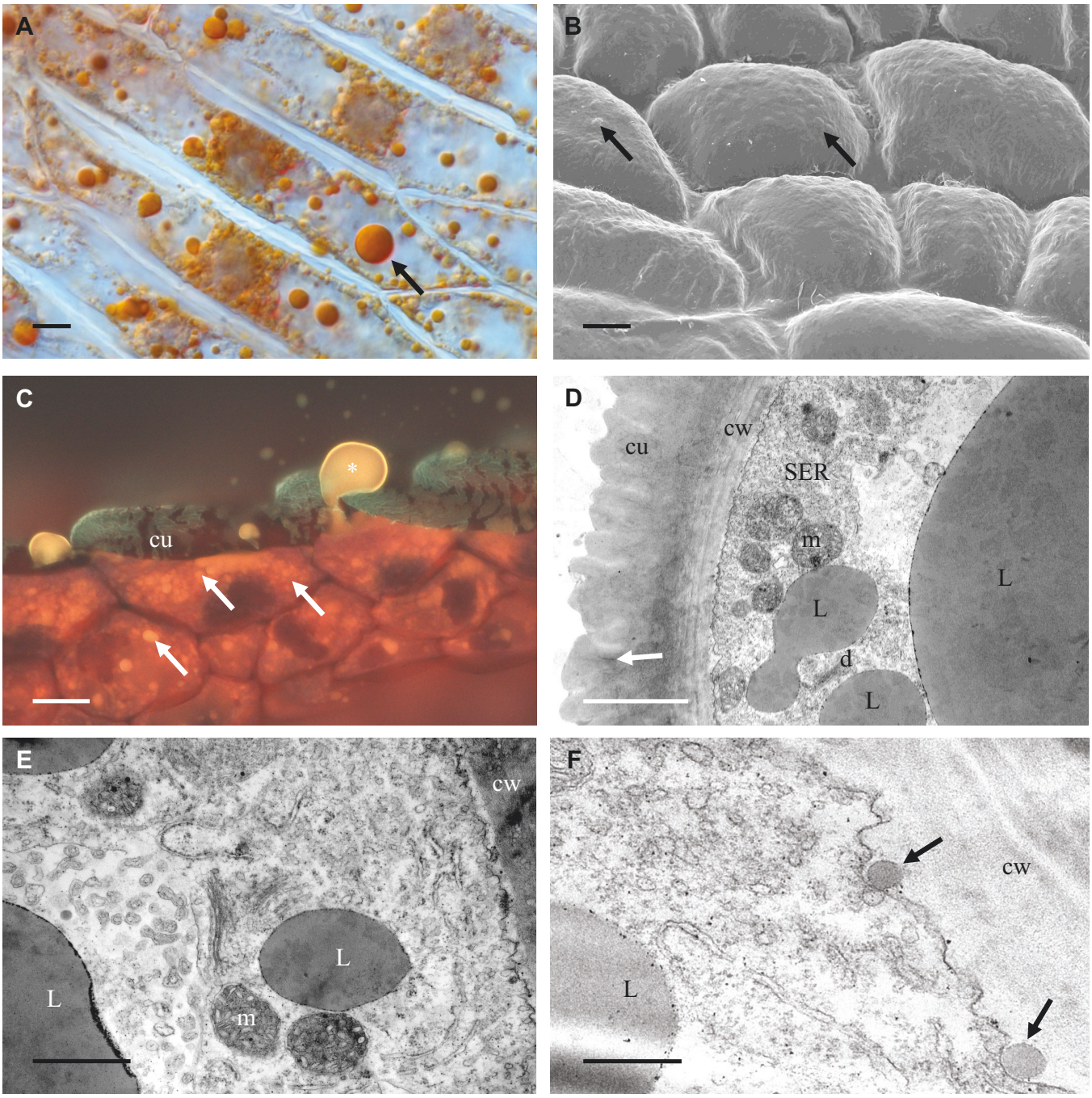

Figure 4. Floral histochemistry of *B. picturatum* and *B. rothschildianum*, and ultrastructure of *B. bicolor* and *B. rothschildianum*. A, Epidermal cells of lateral sepal of *B. rothschildianum* (KLD 201712) stained with Sudan IV to show intracellular droplets of volatile compounds (arrow). B, SEM of labellar epidermal cells of *B. picturatum* (KLD 201714) showing cuticular blisters (arrows). C, Adaxial labellar epidermal cells (median groove) of *B. rothschildianum* stained with NR and observed under UV. Note the large yellow droplet of volatile oil on the adaxial labellar surface (asterisk) and numerous smaller intracellular droplets (arrows). D, TEM of adaxial labellar epidermal trichome cell of *B. bicolor* (KLD 201711) showing relatively thick, striate cuticle with feint micro-channels (arrow), together with smooth endoplasmic reticulum, lipid bodies, dictyosomes (Golgi bodies) and mitochondria. E, TEM of labellar epidermal cell of *B. bicolor* (KLD 201711) containing large lipid droplets, numerous vesicles, and smooth endoplasmic reticulum profiles, together with mitochondria and dictyosomes. Note the undulating profile of the plasmalemma and the close juxtaposition of dictyosome (Golgi body), smooth endoplasmic reticulum, and vesicles to form the GERL complex. F, TEM of labellar epidermal cell of *B. rothschildianum* (KLD 201712). Note the presence of small lipid droplets (arrows) in the periplasmic space, and the undulating plasmalemma overlying the cell wall projections. Scale bars: A–C, 10 μm; D, 2 μm; E, 1 μm; F, 0.5 μm. KEY: cu = cuticle; cw = cell wall; d = dictyosome (Golgi body); L = lipid droplet; m = mitochondrion; SER = smooth endoplasmic reticulum.

but were not able to discriminate *B. rothschildianum* from *B. pecten-veneris*, *B. longiflorum*, or *B. picturatum* (Fig. 5A). It was also not possible to discriminate between *B. longiflorum* and *B. pecten-veneris* on the basis of the whole VOC profile. Some of the lack of discrimination may be due to the variability across replicates of *B. rothschildianum* seen in the larger 95% confidence

Table 2. Summary of floral morphology and anatomy.

Taxon	Fragrance	Dorsal sepal	Lateral sepals	Petals	Labellum	Column	Stelidia	Anther cap
B. bicolor Lindl. Accession number KLD 201711. Accessions KLD 201809 and KLD 201810 were similarly coloured.	Although this species is considered by many to produce a sweet fragrance, that of the particular clone investigated here (KLD 201711), based on the findings of three independent witnesses, is distinctly malodorous, smelling mildly of faeces. For general features see (Fig. 1I).	In KLD 201711, pale yellow striped purple-red proximally and spotted purple-red distally with a darker purple-red apex.	Pale yellow striped purple-red throughout, twisted and lack dark apices. Sunken trichomes are present on the abaxial surfaces.	Similar in colour to the dorsal sepal. Sunken trichomes are present on the abaxial surfaces of the petals.	Mobile, pale yellow, flushed orange. Proximally, it is spotted red, both adaxially and abaxially and has a very wide median labellar groove (Fig. 1I). The labellar secretion produced by accession KLD 201711 has a slightly bitter taste and is glucose-negative. It appears to be produced adaxially on the labellum, on the blackish area located at the base of the lateral lobes of the labellum, and collects on the claw or ligament of the column-foot, occurring also towards the apices of the lateral sepals. The labellum is papillose, the conical papillae bearing a striate cuticle.	Pale yellow spotted red, but more uniformly red proximally.	Downwardly curved and white.	Green.

Table 2. Continued

Taxon	Fragrance	Dorsal sepal	Lateral sepals	Petals	Labellum	Column	Stelidia	Anther cap
B. eberhardtii (Gagnep.) Seidenf. Acc No KLD 201208	Considered by some authorities to be conspecific with *B. longiflorum*, this species also lacks a strongly perceptible fragrance. For general features see (Fig. 1A).	Based on accession KLD 201208, the dorsal sepal is white, heavily spotted with dark rose and has a laciniate purple-black apex from which arises a terminal, clavate, purple-black, mobile, hair-like appendage.	Relatively wide compared to their length, white, heavily spotted with dark rose. Twisted such that their morphological abaxial surfaces are uppermost and are fused longitudinally by their margins to form a longitudinal groove (Fig. 1A). Silvery residues of secreted material occur on the surface of the lateral sepals.	Uniformly purple-pink, again with laciniate, purple-black apices and purple-black, terminal, clavate, hair-like appendages. Toward the laciniate apex of the petal, the ground parenchyma contains spherical idioblasts, and these appear to coincide with round clusters of epidermal papillae on the adaxial surface of the petal. The epidermal papillae of the petals have a finely striate cuticle and pointed or rounded apices.	Mobile and purple, with a moderately wide and deep median longitudinal groove or sulcus, and prominent lateral lobes (Fig. 1A). Silvery residues of secreted material occur along the length of this groove. SEM reveals that this secreted material often obfuscates the topography of the papillose adaxial epidermis of the labellum (Fig. 3A).	White finely spotted rose.	Forwardly projecting and white, spotted rose.	Yellow.

Table 2. Continued

Taxon	Fragrance	Dorsal sepal	Lateral sepals	Petals	Labellum	Column	Stelidia	Anther cap
B. fascinator (Rolfe) Rolfe var. *semi-album* Accession number KLD 201820	Foetid fragrance. For general features see (Fig. 1B).	Typical flowers of this foetid species are generally pale yellow-green overlaid to varying degrees with red, reddish-brown or purple, but those of var. semi-album KLD 201820 are very differently coloured (Fig. 1B). The dorsal sepal is pale yellow-green peppered with brown, the pointed apex arising abruptly from the lamina and bearing a tuft of purple paleae. The margins of the dorsal sepal are white, hyaline, and fringed with purple paleae. No indication of surface secretion residues on the dorsal sepal.	Pale yellow-green and distinctly verrucose, once more peppered with brown or a darker green which corresponds with the apices of individual verrucae. Lateral sepals twisted such that their morphological abaxial surfaces are uppermost and are fused longitudinally by their margins to form a longitudinal groove (Fig. 1B). However, the twisting here is not as distinct as in many species as it occurs close to the receptacle and is partly obscured by the lamina of the lateral sepals. The outer (abaxial) surface of the lateral sepals is verrucose, the verrucae being papillose and bearing stomata and sunken trichomes.	Pale yellow-green, heavily speckled with purple-brown and bearing marginal, purple paleae and a terminal tuft of similar paleae (Figs 1B, 1J). No indication of surface secretion residues on petals.	Mobile, and adaxially brown-red to purple-black, except for the floor of the wide and deep median longitudinal groove (Fig. 1B), which is greenish-yellow. Abaxially the labellum is pale yellow with large brown-red spots. For general floral anatomy see (Fig. 3B). Secreted material occurs on the adaxial surface.	Yellow, speckled brown-red.	White and projecting forward and downward.	White with a purple apex.

Table 2. Continued

Taxon	Fragrance	Dorsal sepal	Lateral sepals	Petals	Labellum	Column	Stelidia	Anther cap
B. longibrachiatum Z.H. Tsi Accession number MP1	No data available.	Pale yellow-green outlined with purple-red along the innermost edge of the margins, and puncto-striate, marked with confluent purple-red blotches arranged lengthwise, forming lines. White fimbriae tend only to occur apically on the dorsal sepal. In both dorsal sepal and petals, the terminal fimbriae are longer than elsewhere. The margins of the dorsal sepal are ciliate. Surface lipid-like secretion is present, particularly at the margins of the lateral sepals.	Yellow-green, marked or heavily suffused with red, giving a brownish appearance. Twisted such that their morphological abaxial surfaces are uppermost and are fused longitudinally by their margins to form a longitudinal groove. The epidermal cells are flattened or slightly papillose and have a finely striate cuticle. Numerous stomata are present on both surfaces of the lateral sepals and are particularly densely distributed towards their apices. Stomata do not appear to be associated with residues of secreted material present on the surface of lateral sepals.	Similar to the dorsal sepal, but margins are densely fringed with white fimbriae. In both dorsal sepal and petals, the terminal fimbriae are longer than elsewhere.	Mobile and yellow, adaxially heavily suffused with red, with relatively shallow and narrow median longitudinal groove lined with cuboidal or palisade-like cells. No indication of surface secretion residues.	White (yellow terminally), and spotted with purple-red.	Yellow, marked red, long, strongly falcate and pointing forward and downward.	Yellow.

Table 2. Continued

Taxon	Fragrance	Dorsal sepal	Lateral sepals	Petals	Labellum	Column	Stelidia	Anther cap
B. longiflorum Thouars Accession number KLD 201322. Accession MP6 was similar.	Closely resembling *B. eberhardtii*, the flowers of *B. longiflorum* are much more variable in colour. Lateral sepals are narrower relative to length than in *B. eberhardtii*. No perceptible fragrance.	Pale yellow in KLD 201322, heavily spotted purple-red, with a uniformly purple apex which has projections and bears a terminal, almost black, clavate appendage.	Pale yellow heavily suffused and spotted with deep rose-pink. Twisted such that their morphological abaxial surfaces are uppermost and are fused longitudinally by their margins to form a longitudinal groove.	Uniform dark purple-red and apically laciniate, again with an almost black, clavate terminal projection.	Mobile labellum rose and possesses a moderately narrow and shallow sulcus, and well-defined lateral lobes. In this accession, the sulcus or median labellar groove was clearly fluid-filled and droplets were also visible on the adaxial surface of the labellum.	White, spotted purple-red.	Forwardly projecting with down-turned rose-coloured tips.	White.
B. longiflorum Thouars Accession number KLD 201414	Although accession KLD 201414 (Fig. 1C) has previously been investigated (Stpiczyńska *et al.* 2018a), here we use it for comparative purposes. Here, the flowers (Fig. 1C) are very similar in structure and coloration to KLD 201322, but the general ground colour is greenish-white, heavily marked dark pink to purple-brown. No perceptible fragrance.	Similar to KLD 201322. Clavate, black appendages arise from dorsal sepal (Fig. 1C).	Similarly coloured to the dorsal sepal. Twisted such that their morphological abaxial surfaces are uppermost and are fused longitudinally by their margins to form a longitudinal groove (Fig. 1C). They are coated with silvery residues of secreted material.	Clavate, black appendages arise from the black-tipped petals.	Mobile, dark pink to purple-brown, downwardly curved, and almost centric distally in transverse section (Fig. 1C). Silvery secretory residues associated with the narrow sulcus, but tested negative for glucose on days 2 and 6 of anthesis.	Similar to above.	Similar to above.	Similar to above.
B. longiflorum Thouars Accession number KLD 201802	No perceptible fragrance. For general features see (Fig. 1D).	Pale yellow spotted rose, with a uniformly coloured rose apex and a terminal, clavate, purple appendage (Fig. 1D).	Similarly coloured to the dorsal sepal, though much more yellow distally (Fig. 1D). Twisted such that their morphological abaxial surfaces are uppermost and are fused longitudinally by their margins to form a longitudinal groove.	Pale yellow, heavily spotted rose, fimbriate to laciniate, with a uniformly coloured apex bearing a terminal, clavate, purple appendage (Fig. 1D). As in *B. eberhardtii*, apically, spherical idioblasts are present in the petal, and these are prominent, even in preserved material at low magnification.	Yolk-yellow heavily spotted with brownish-pink, with a relatively narrow and shallow sulcus (Fig. 1D).	White, heavily spotted rose.	Forwardly projecting with downwardly pointing tips.	Yellow.

Table 2. Continued

Taxon	Fragrance	Dorsal sepal	Lateral sepals	Petals	Labellum	Column	Stelidia	Anther cap
B. ornatissimum (Rchb.f.) J.J. Sm. Accession number KLD 201821	Foetid fragrance. For general features see (Fig. 1F).	Dirty pale yellow, heavily spotted with purple-red, the spots arranged in rows and becoming more confluent toward the apices, which are entirely purple-red and bear several long, dark purple, hair-like projections, the central one being longer than the others (Fig. 1F). Both abaxial and adaxial epidermal cells of the dorsal sepal are smooth, becoming papillose toward the distal part of the organ, and sunken trichomes are present on both surfaces.	Dirty pale yellow, heavily spotted with purple-red, the spotting being larger and denser adaxially than abaxially. Twisted such that their morphological abaxial surfaces are uppermost and are fused longitudinally by their margins to form a longitudinal groove (Fig. 1F).	Identically coloured to the dorsal sepal, with rows of purple spots and purple apices, as well as an apical tuft of dark purple, hair-like projections, the central one being longer than the others (Fig. 1F). Both abaxial and adaxial epidermal cells are similar to those of the dorsal sepal.	Mobile and purple, spotted dark purple to black, with a moderately wide and deep median longitudinal groove (Fig. 1F).	Dirty pale yellow to greenish-yellow, heavily speckled with purple-red.	No pronounced stelidia appear to be present.	Yellow.

Table 2. Continued

Taxon	Fragrance	Dorsal sepal	Lateral sepals	Petals	Labellum	Column	Stelidia	Anther cap
B. pecten-veneris (Gagnep.) Seidenf. Accession number KLD 201318. Accession MP2 was similar.	Another variable species, the general colour ranging from yellow to orange, with no perceptible fragrance. For general features of the yellow form, see (Fig. 1E).	Yolk-yellow abaxially in KLD 201318, white adaxially, with orange fimbriate margins. Terminal tuft present of short appendages approaching paleae in form (Fig. 1E). Atypical, multiseriate, multicellular trichomes distributed along the margins of the dorsal sepal and petals (Fig. 2A-C), and these possess a striate cuticle (Fig. 2D).	Yolk-yellow proximally, fading to off-white distally. Twisted such that their morphological abaxial surfaces are uppermost and are fused longitudinally by their margins to form a longitudinal groove (Fig. 1E).	Yolk-yellow abaxially, white adaxially, with orange fimbriate margins (Fig. 1E). Atypical multiseriate, multicellular trichomes, such as those found along the margins of the dorsal sepal, also occur on the petals and at their bases (Fig. 2C).	Mobile, white distally, pale orange proximally, the sulcus narrow and shallow (Fig.1E). Although parts of the labellum are glabrous, others are papillose, possessing conical papillae.	White to pale yellow.	White to pale yellow.	White to pale yellow.

Table 2. Continued

Taxon	Fragrance	Dorsal sepal	Lateral sepals	Petals	Labellum	Column	Stelidia	Anther cap
B. picturatum (Lodd.) Rchb.f. Accession number KLD 201714. Accession BN was similar.	Distinguished from the very similar *B. pseudopicturatum* (Garay) Sieder & Kiehn in that its petals taper to a point and bear prominent terminal hairs. Foetid odour. For general features see (Fig. 1G).	Pale yellow, spotted dark purple with a dark purple or red apex and a black, clavate, terminal appendage (Fig. 1G).	Similarly coloured to dorsal sepal, more intensely adaxially. Twisted such that their morphological abaxial surfaces are uppermost and are fused longitudinally by their margins to form a longitudinal groove (Fig. 1G).	Similarly coloured, with dark purple-black or red apices (Fig. 1G), but the spotting is more confluent and the margins fimbriate.	Mobile, arcuate, dark purple-black with well-defined lateral lobes and a relatively wide and deep median longitudinal groove or sulcus (Fig. 1G). The adaxial epidermis in the median part of the labellum comprises flat to slightly convex cells, whereas marginally these cells are papillose (short, squamous papillae). A film of shiny, secretory residue was present on the adaxial surface of the mid-lobe of the labellum, about half way along its length. This film lacked a sweet taste and was mildly bitter. Beneath the epidermis occur 2-3 layers of small, densely packed subepidermal cells (hypodermis), together with aerial parenchyma (aerenchyma). Embedded in the latter tissue are several vascular bundles. Abaxial epidermal cells are more papillose than adaxial epidermal cells. Similar labellar anatomy occurs in *B. fascinator* var. *album* (Fig. 3B).	Heavily mottled dark purple.	White, straight and forwardly and downwardly projecting.	Yellow.

Table 2. Continued

Taxon	Fragrance	Dorsal sepal	Lateral sepals	Petals	Labellum	Column	Stelidia	Anther cap
B. rothschildianum (O'Brien) J.J. Sm. Accession Nos. KLD 201712 and KLD 201713. Accessions MP3 and MP4 were similar.	Flowers of this species vary from red to reddish-brown (Fig. 1H) and are foetid.	Pale yellow, striped brick-red (KLD 201712) or reddish-brown (Fig. 1H - KLD 201713), the apices bearing marginal and terminal purple-red to purple-black paleae which are more concentrated apically. Droplets of secretion occur at the base of the dorsal sepal. The cuticle overlying the epidermal cells of the paleae of the dorsal sepal was sculptured.	Similarly coloured to the dorsal sepal. Twisted such that their morphological abaxial surfaces are uppermost and are fused longitudinally by their margins to form a longitudinal groove (Fig. 1H). Their adaxial surface is more intensely coloured than the abaxial surface. Droplets of secretion occur at the base and uppermost surface of the lateral sepals, as well as on the paleae. The lateral sepals have convex epidermal cells and typical ground parenchyma. The cuticle is striate, and residues of surface material are visible by SEM and FM. Sunken trichomes are also present, particularly on the abaxial surface.	Yellow, striped brick-red or reddish-brown (Fig.1H - KLD 201713), the apices bearing marginal and terminal purple-red to purple-black paleae which are more concentrated apically. SEM revealed that a finely striate cuticle was also present on the epidermal cells of the petals. The cuticle overlying the epidermal cells of the paleae of the petals was sculptured. Scattered, sunken, clavate trichomes comprising a stalk and head, were also present on petals.	Mobile, dark red, heavily spotted darker red distally and purple-black proximally (Fig. 1H). The proximal margins are fimbriate, and the labellum possesses a wide and deep sulcus. Droplets of secretion occur adaxially about half way along the length of the mid-lobe of the labellum and in the median longitudinal groove. The margins of the labellum possess squamous papillose cells or unicellular trichomes (Fig. 3E, F) with a finely striate cuticle. These trichomes often occur in pairs that are tightly adpressed to each other toward their bases, between which occur residues of secreted material (Fig. 3E). This material is also visible using both SEM and FM (Fig. 4C).	Heavily mottled with red.	White with red tips, and downwardly curved.	White with a red apex.

Table 2. Continued

Taxon	Fragrance	Dorsal sepal	Lateral sepals	Petals	Labellum	Column	Stelidia	Anther cap
					Proximally, the adaxial epidermal cells lining the median longitudinal groove are more or less cuboidal to rectangular in transverse section. Elsewhere, the labellar epidermis comprises typical convex cells. The subepidermal parenchyma is more defined at the proximal part of the labellum and beneath this tissue occurs ground parenchyma, which elsewhere almost becomes differentiated into aerenchyma.			

Table 2. Continued

Taxon	Fragrance	Dorsal sepal	Lateral sepals	Petals	Labellum	Column	Stelidia	Anther cap
B. sanguineopunctatum Seidenf. & A.D. Kerr Accession number MP5.	No data available.	White, heavily dotted with linearly arranged, fine, rose spots, more so abaxially than adaxially. Marginally, the dorsal sepal bears dense, white, paleate fimbriae or paleae. The dorsal sepal is ciliate. Stomata are present abaxially and adaxially. Idioblasts, most of which are empty, are also present, but some bundles of raphides were visible in whole-mounts of the organ on careful focusing. Idioblasts lack mucilage.	White, heavily dotted with linearly arranged, fine, rose spots, more so abaxially than adaxially. Twisted such that their morphological abaxial surfaces are uppermost and are fused longitudinally by their margins to form a longitudinal groove. Numerous, single or paired trichomes with secretory 'heads' occur abaxially on the lateral sepals. Stomata are present abaxially and adaxially. Idioblasts, most of which are empty, are also present, but some bundles of raphides were visible in whole-mounts of the organ on careful focusing. Idioblasts lack mucilage.	White, heavily dotted with linearly arranged, fine, rose spots, more so abaxially than adaxially. Marginally, the petals bear dense, white, paleate fimbriae or paleae. The petals are ciliate. Stomata are present abaxially and adaxially. Idioblasts, most of which are empty, are also present, but some bundles of raphides were visible in whole-mounts of the organ on careful focusing. Idioblasts lack mucilage.	Yellow with a deep and wide median longitudinal groove. The glistening of the labellar groove indicated the probable presence of secreted material. The parenchymatous ground tissue, which forms the bulk of the labellum, has an extensive intercellular space system.	White.	White, short, straight, and forwardly pointing.	Cream.

Table 3. Summary of labellar features and occurrence of surface secretions.

Taxon	Labellar secretion present	Labellar secretory cells	Labellar cuticle	Dorsal sepal	Lateral sepals	Petals	Tepal appendages
B. bicolor Lindl.	+	Cuboidal with lipid droplets (Fig. 4D, E).	Micro-channels present in labellar cuticle (Fig. 4D).	Surface secretion present, lipid mainly absent.	Surface secretion with lipid present.	Surface secretion present, lipid mainly absent.	
B. eberhardtii (Gagnep.) Seidenf.	+ (Fig. 3A) with small quantities of protein.	+/− rectangular with lipid droplets.	No blistering observed.	Lipid present.	Surface secretion present with lipid.	Surface secretion present with lipid towards tips of petals.	
B. fascinator (Rolfe) Rolfe var. *semi-album*	+	Cuboidal to slightly rectangular with lipid droplets.	Blistered with subcuticular lipid.	No visible surface secretion.	Surface secretion with lipid.	No visible surface secretion, possibly a little at base.	Paleae of dorsal sepal and petals with small quantities of lipid (Fig. 1J).
B. longibrachiatum Z.H. Tsi	+	Cuboidal to almost palisade-like with lipid droplets (Fig. 3C).	Blistered.	Possibly some surface secretion, lipid present.	Possibly some surface secretion, lipid present.	Lipid present, also in marginal cilia.	
B. longiflorum Thouars	+ with small quantities of protein.	Cuboidal to slightly rectangular with lipid droplets (Fig. 3D).	No blistering observed.	Surface secretion present.	Surface secretion with lipid present.	Lipid present, also in marginal laciniae.	Clavate appendages with lipid.
B. ornatissimum (Rchb.f.) J.J. Sm	+	Cuboidal with lipid droplets.	No blistering observed.	Secreted material present, lipid seemingly absent.	Lipid present, especially at margins.	Secreted material present at base, lipid seemingly absent.	
B. pecten-veneris (Gagnep.) Seidenf.	No obvious surface secretion, except for minute droplets, but labellum stains selectively with Sudan III.	Cuboidal with lipid droplets.	No blistering or cuticular pores.	No obvious surface secretion, except for minute droplets, but lipid present especially in oleiferous trichomes and marginally (Fig. 2A, B, D).	No obvious surface secretion, except for minute droplets.	No obvious surface secretion, except for minute droplets, but lipid present especially in oleiferous trichomes and marginally (Fig. 2C, E, H).	

Table 3. Continued

Taxon	Labellar secretion present	Labellar secretory cells	Labellar cuticle	Dorsal sepal	Lateral sepals	Petals	Tepal appendages
B. picturatum (Lodd.) Rchb.f.	+	Cuboidal with lipid droplets.	Blistered (Fig. 4B).	Surface secretion present with lipid, especially marginally.	Surface secretion present with lipid.	Surface secretion present, lipid seemingly absent.	Clavate appendage of dorsal sepal with few lipid droplets.
B. rothschildianum (O'Brien) J.J. Sm.	+ (Fig. 4C).	Cuboidal to rectangular with lipid droplets (Fig. 4F), also present in trichomes (Fig. 3E, F).	Blistered (Fig. 4C). Microchannels present in cuticle of labellar trichomes.	Surface secretion present with lipid.	Surface secretion present with much lipid and cuticular blistering. Oil droplets present in epidermal cells (Fig. 4A).	Surface secretion present with lipid.	Paleae of dorsal sepal and petals with distension but no rupturing of cuticle and no surface secretion. Clavate appendage of dorsal sepal with more lipid droplets than other species investigated.
B. sanguineopunctatum Seidenf. & A.D. Kerr	+	Cuboidal to conical with lipid.	No blistering visible.	Surface secretion with lipid present, also in marginal cilia.	Surface secretion present, lipid seemingly absent.	Small amounts of surface secretion present with lipid, also in marginal cilia.	

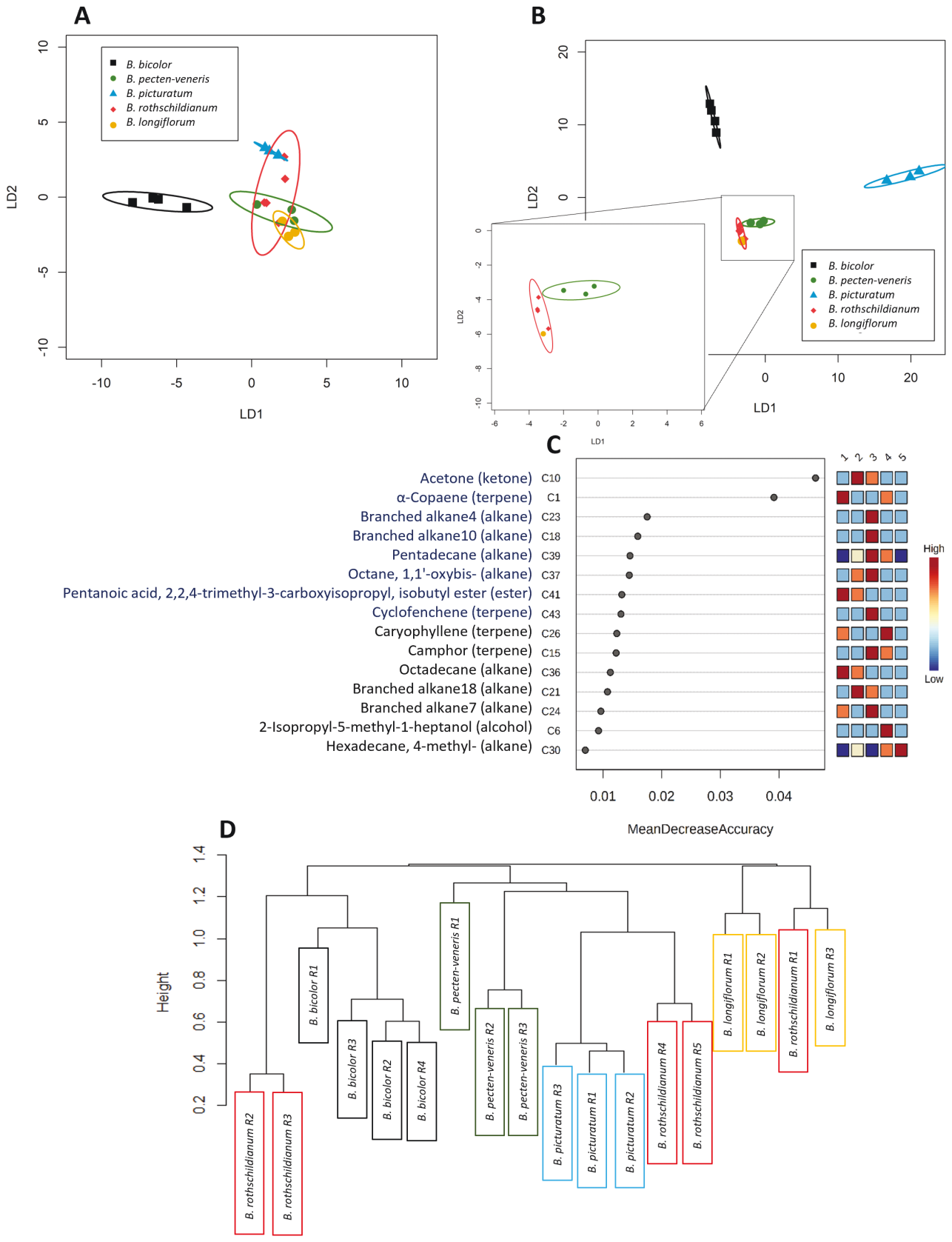

Figure 5. Discrimination of *Bulbophyllum* species based on VOC profiles. A, Canonical analysis of principal coordinates (CAP) based on whole profile of 44 VOCs. B, CAP based on the top eight VOCs identified in random forest analysis. C, Random forest analysis identifying the top 10 VOCs providing the greatest discrimination across species. D, Optimal hierarchical clustering of whole VOC profile using Flashclust in R. Ellipses in A and C represent the 95% confidence interval. Percentage of correct classifications for A, 83% ($P = 1$), $m = 3$ and C, 78% ($P = 1$), $m = 5$.

ellipse for this species (Fig. 5A) and the distribution of the replicates across the hierarchical tree (Fig. 5D). Hence, random forest algorithms were used to assess whether a subset of the VOCs had greater discriminatory power (Fig. 5C). The top 15 discriminatory VOCs based on random forest analysis comprised eight alkanes, four terpenes, one ester, ketone, and alcohol. The eight most discriminatory VOCs still showed discrimination among *Bulbophyllum* species (PERMANOVA $P < 0.05$, $R^2 = 0.017$), and linear discriminant profiles based on CAP also showed discrimination among most *Bulbophyllum* species, but not between *B. rothschildianum* and *B. longiflorum* (Fig. 5B).

DISCUSSION

Vermeulen (in Pridgeon *et al.* 2014) lists the morphological characters that distinguish members of sections *Cirrhopetalum* and *Cirrhopetaloides* (summarized in Supporting Information, Table S1). One character in particular has been considered useful in this respect—the presence of a tooth on the adaxial surface of the stelidia in members of sect. *Cirrhopetalum*. However, this account also states that for *Cirrhopetalum*, a tooth may or may not be present along the upper and/or lower margin of the stelidia, and that for *Cirrhopetaloides*, there is usually a tooth or wing along the upper and lower margins. Given such variation and overlap of characters, let alone their small size, we consider the sole use of the adaxial tooth, to the exclusion of other potentially useful characters, to distinguish between these sections, unsafe, especially in small-flowering species. Indeed, the specimens of *B. ornatissimum* that we examined possessed only poorly defined stelidia (Table 2), and had there even been any adaxial tooth present, it would have been extremely difficult to detect. We therefore recommend that the adaxial tooth be used for taxonomy only in conjunction with other characters, preferring the approach adopted by Hu *et al.* (2020) of grouping all these species into one '*Cirrhopetalum* alliance', an approach that is supported both by comparative anatomy and VOC analyses.

Regardless of differences in gross floral morphology, generally the floral anatomy of the '*Cirrhopetalum* alliance' resembles that of other sections of *Bulbophyllum*, Asian, African, and Neotropical. The labellum possesses a longitudinal median groove or sulcus, a single-layered adaxial and abaxial epidermis, together with a several-layered subepidermal region overlying ground parenchyma (sometimes approaching aerenchyma) containing collateral vascular bundles and often idioblasts with bundles of raphides (Davies and Stpiczyńska 2014, Nunes *et al.* 2014, 2015, 2017a, Stpiczyńska *et al.* 2015, 2018a, b, Stpiczyńska and Davies 2016, Wiśniewska *et al.* 2018, 2019). The sulcus is lined with secretory, adaxial epidermal cells, which, in the '*Cirrhopetalum* alliance', are usually cuboid to slightly rectangular in transverse section. However, in contrast to the other species of *Bulbophyllum* examined here, this secretory tissue, in *B. longibrachiatum*, occasionally contains somewhat more elongate epithelial cells approaching the palisade-like secretory cells of species of the Asian sect. *Racemosae* (Davies and Stpiczyńska 2014), African *B. schinzianum* (sect. *Ptiloglossum*—Stpiczyńska *et al.* 2015), and Neotropical sect. *Napelli* (Nunes *et al.* 2015), thus indicating parallelism and reflecting a degree of secretory tissue specialization. In most sections of *Bulbophyllum* studied to date (including the '*Cirrhopetalum* alliance'), the secreted material from these cells mainly contains lipid (e.g. Nunes *et al.* 2014, 2015, Kowalkowska *et al.* 2015, 2017, Stpiczyńska *et al.* 2015, 2018b), although that of sect. *Racemosae* is unusual in that it comprises protein-laden mucilage, and lipid is absent (Davies and Stpiczyńska 2014, Stpiczyńska and Davies 2016). Remarkably, unlike the other taxa investigated, secreted, lipid-rich material on the labella of *B. eberhardtii* and *B. longiflorum* also contains small quantities of protein, strengthening the hypothesis that these two taxa may be conspecific, as asserted by some authorities (e.g. WCSP 2022), or at least indicate that their respective secretory biochemical pathways have evolved along similar routes. The labellar cuticle is often blistered, and cuticular micro-channels may sometimes be present, as recorded for other representatives of the genus (e.g. Davies and Stpiczyńska 2014, Nunes *et al.* 2014, 2015, 2017a, Kowalkowska *et al.* 2015, 2017, Stpiczyńska *et al.* 2015, 2018a, b, Stpiczyńska and Davies 2016, Wiśniewska *et al.* 2018, 2019). Furthermore, projections may also be present on the cell wall, as first observed by Kowalkowska *et al.* (2015).

One noteworthy character, described here for the first time, is the abundantly oleiferous, marginal trichomes of the dorsal sepals and petals of *B. pecten-veneris*. These were not seen in other species investigated. Although copiously oleiferous trichomes have previously been described for the African species *B. schinzianum* (Stpiczyńska *et al.* 2015) and *B. saltatorium* (Stpiczyńska *et al.* 2018b, both members of sect. *Ptiloglossum*), they occur on the labellum, and are unicellular (and capitate in *B. saltatorium*), whereas those of Asian *B. pecten-veneris* are atypical, multiseriate, and multicellular. It is proposed that the intracellular lipid droplets of both types of trichome may function as precursors of volatile compounds and/or as food rewards. However, the marginal distribution of trichomes would perhaps favour the former hypothesis.

Although we have been able to identify VOC-producing cells and tissues, typical, true osmophores (multicellular, fragrance-producing glandular structures), as described by Vogel (1990), an anatomical term which has been frequently misapplied, are seemingly lacking. However, Kowalkowska *et al.* (2015) have proposed that the clavate appendages borne terminally on perianth segments are in fact osmophores, their cuticle becoming blistered. Indeed, the clavate appendages and paleae associated with the perianth segments of our material also contained lipid droplets, but these were relatively few and small compared with those of labellar and lateral sepal tissue, indicating that it is these last organs that are probably the primary source of volatile compounds. The hinged labellum and various appendages to the perianth segments have been referred to as 'flickering bodies' from the German Flimmerkörper, or 'vibratile bodies' (Vogel 2001, Kowalkowska *et al.* 2015) since they move in the slightest breeze or air currents, and have long been claimed to be involved in the attraction of insect pollinators. Similarly, the paleae also move in air currents and perhaps help disperse volatile compounds, as perhaps do other floral oleiferous epidermal structures such as fimbriae and laciniae, especially those along the margins of perianth segments.

Despite published differences in the gross floral morphology of sections *Cirrhopetalum* and *Cirrhopetaloides,* the floral anatomy/micromorphology of sect. *Cirrhopetalum*, as currently circumscribed, lacks any characters or combination of characters unique

to this taxon. Indeed, many of these characters are shared by species currently assigned to sect. *Cirrhopetaloides*, and by members of other sections native to Asia, Africa, and the Neotropics (e.g. Davies and Stpiczyńska 2014, Nunes *et al.* 2014, 2015, 2017a, Stpiczyńska *et al.* 2015, 2018a, b), and are indicative of convergence or parallelism. This indicates the need for further taxonomic revision based on a more biochemical approach.

VOC profiles among the *Bulbophyllum* species investigated

Previous investigations have shown that the VOC profiles of *Bulbophyllum* species can vary considerably. For example, ketones, aldehydes, alcohols, and aromatic compounds dominate those of fly-pollinated species, whereas bee-pollinated species emit more terpenes (Silva *et al.* 1999). VOC profiles can also differ between fly-pollinated orchids (Silva *et al.* 1999), and 'daciniphilous' *Bulbophyllum* orchids can be divided into three groups based on whether methyl eugenol, zingerone [4-(4-hydroxy-3-methoxyphenyl)-2-butanone], or raspberry ketone [(4-(4-hydroxyphenyl)-2-butanone] is the major component of their respective VOC profile (Tan and Nishida 2000, 2005, Nakahira *et al.* 2018), thus reflecting pollination by different fly species. Acetic, butyric, 2-methylbutyric, and valeric acid occur in other species, in conjunction with *N*-methyl and *N,N*-dimethyl derivatives of acetamide and formamide, which contribute to the malodorous 'stench' of *B. graveolens* (Kaiser 1993). Butyric acid is also a component of the carrion-like odour produced by the labellum of *B. fascinator*, whereas caryophyllene epoxide contributes to a pleasant woody scent associated with the sepals, caryophyllene being a major component (55%) of the overall gas chromatography with mass spectrometry profile (Kaiser 1993). The fragrance of *B. lobbii* contained 28 components, mainly linalool and (*E*)-ocimine and its derivatives, whereas that of *Bulbophyllum gracillimum* comprised acetic acid, geranylacetone, (*Z*)-3-hexenol, (*Z*)-3-hexenyl tiglate, indole, isoleucine methyl ester, and nonanal (Kaiser 1993).

Perhaps, owing to the combination of collection of headspace VOCs onto TD tubes and the use of a highly sensitive time-of-flight gas chromatography with mass spectrometry system, a larger number of VOCs were detected in the species investigated here compared to previous studies of VOCs from the genus *Bulbophyllum* (Kaiser 1993, Silva *et al.* 1999, Tan and Nishida 2000, Tan *et al.* 2002, Humeau *et al.* 2011, Nakahira *et al.* 2018, Katte *et al.* 2020). A few VOCs detected here were also found in the aroma profiles of other *Bulbophyllum* species, including caryophyllene and humulene, also found in *B. variegatum* (Humeau *et al.* 2011). Overall, fewer VOCs (five) were found in the aroma of *B. longiflorum* than in the other species tested here, consistent with the lack of perceived fragrance for the flowers of this species. Few VOCs were also detected in the profile from flowers of *B. bicolor*: some of them are described as having a woody/spicy odour (α-copaene and humulene), while others have a fruity fragrance (butyl acetate) that would fit with the sweet fragrance described previously. Although the profiles across the five species analysed were not completely distinct, the whole VOC profile clearly discriminated between *B. bicolor* and the other four species. Moreover, statistical analyses indicated that subsets of VOCs were able to discriminate across most of the species. This might suggest different pollinator assemblages for these species, as previously described for other closely related *Bulbophyllum* species (Tan and Nishida 2000, Nakahira *et al.* 2018). They might also provide a rapid method for discriminating between taxa such as certain species of *Ophrys* that possess very similar floral morphology (Mant *et al.* 2005, Stökl *et al.* 2009), with the caveat that fragrance profile can change with the age of the flower and diurnally, as well as relative to geographic ranges, drought, and global and other environmental changes, both across spatial and temporal scales (Farré-Armengol *et al.* 2013, Burkle and Runyon 2017, Delle-Vedove *et al.* 2017, Jaworski *et al.* 2022).

The discrimination of species according to VOC profiles differed from the phylogeny inferred from the DNA markers (Hu *et al.* 2020). *Bulbophyllum bicolor* was clearly distinct from the other species both using the whole VOC profile and a subset of VOCs, whereas according to Hu *et al.* (2020), it belongs in the same clade as *B. rothschildianum*. The VOC profile of *B. pectenveneris*, which according to Hu *et al.* (2020) is the most distantly related species to the other four considered here, and the only species to possess atypical oleiferous labellar trichomes, was, by contrast, not discriminated from that of *B. rothschildianum* or *B. longiflorum*. These marked differences between the VOC distinctness and sequence-based phylogenies are consistent with a recent diversification, and indicate that differences in pollinator assemblages have driven change in VOC profile across this closely related group of species.

VOC composition, as well as reflecting divergent evolutionary pathways, may also be due to pollinator specificity and age of the flower. Furthermore, floral morphology is also closely related to pollinator specificity and Pansarin and Pansarin (2011) and Aguiar *et al.* (2012) have demonstrated that geographically widely distributed orchid species may also display very different pollination syndromes, involving different pollinator species, and this is reflected both in the composition of the food rewards and the fragrances that they produce.

In conclusion, neither the anatomical nor VOC analyses of this study support the separation of sect. *Cirrhopetalum* and sect. *Cirrhopetaloides*. Expanded taxon sampling for VOCs along with detailed information on pollinator species will be required to achieve a comprehensive understanding of the evolution of pollination syndromes in *Bulbophyllum*. Until then, there is little evidence to justify the distinction between sect. *Cirrhopetalum* and sect. *Cirrhopetaloides* based on these characters, amplifying previous calls (Hu *et al.* 2020) that the '*Cirrhopetalum* alliance' is in need of revision.

SUPPLEMENTARY DATA

Supplementary data is available at *Botanical Journal of the Linnean Society* online.

FUNDING

The authors are grateful to the Stanley Smith (UK) Horticultural Trust (grant to K.L.D.) and to the National Science Centre, Poland (grant number 2014/15/B/NZ8/00210 to M.S.) for partly funding this work.

ACKNOWLEDGEMENTS

TEM studies were performed at the Laboratory of Electron Microscopy, Nencki Institute of Experimental Biology, Warsaw,

Poland. TEM facilities were installed for the project and sponsored by EU Structural Funds (SPO WWKP_1/1.4.3/2/2005/102/22 2/562/U). The authors are grateful to Agnieszka Krzyk (Botanic Garden, University of Warsaw, Poland) for tissue preparation, to Julita Nowakowska (Laboratory of Electron-Microscopy, University of Warsaw) and to Szymon Suski and Henryk Bilski (Nencki Institute of Experimental Biology) for assistance with SEM and TEM, respectively. VOC and DNA analyses were undertaken at the School of Biosciences, Cardiff University, UK. Thanks are also due to J.J. Vermeulen for helping to confirm the identity of some of the species investigated, to Malcolm Perry (Bristol, UK) and the staff of Burnham Nurseries Ltd (Newton Abbot, UK) for providing some of the plant material, and to Alan Gregg (Swansea Botanical Complex, UK) for help in assembling the manuscript.

CONFLICT OF INTEREST

None declared.

DATA AVAILABILITY

The data underlying this article are available in Home - Nucleotide - NCBI (nih.gov) at https://www.ncbi.nlm.nih.gov/nucleotide/ and can be accessed with accession numbers: OM687356, OM687357, OM687358, OM687359, OM687360, OM687361, OM687362, OP451904, OP451905, OP451906, OP451907, OP451908.

REFERENCES

Aguiar JMRBV, Pansarin LM, Ackerman JD *et al*. Biotic *versus* abiotic pollination in *Oeceoclades maculata* (Lindl.) Lindl. (Orchidaceae). *Plant Species Biology* 2012;**27**:86–95.

Anderson MJ, Legendre P. An empirical comparison of permutation methods for tests of partial regression coefficients in a linear model. *Journal of Statistical Computation and Simulation* 1999;**62**:271–303. https://doi.org/10.1080/00949659908811936

Anderson MJ, Willis TJ. Canonical analysis of principal coordinates: a useful method of constrained ordination for ecology. *Ecology* 2003;**84**:511–25.

Ayasse M, Stökl J, Francke W. Chemical ecology and pollinator-driven speciation in sexually deceptive orchids. *Phytochemistry* 2011;**72**:1667–77. https://doi.org/10.1016/j.phytochem.2011.03.023

Brummitt RK, Powell CE. *Authors of Plant Names*. UK: Royal Botanic Gardens, Kew, 1992.

Burkle LA, Runyon JB. The smell of environmental change: using floral scent to explain shifts in pollinator attraction. *Applications in Plant Sciences* 2017;**5**:1600123.

Castañeda-Zárate M, Johnson SD, van der Niet T. Food reward chemistry explains a novel pollinator shift and vestigialization of long floral spurs in an orchid. *Current Biology* 2021;**31**:238–46.e7. https://doi.org/10.1016/j.cub.2020.10.024

Chase MW, Cameron KM, Freudenstein JV *et al*. An updated classification of Orchidaceae. *Botanical Journal of the Linnean Society* 2015;**177**:151–74. https://doi.org/10.1111/boj.12234

Chen L-L, Gao J-Y. Reproductive ecology of *Bulbophyllum ambrosia* (Orchidaceae). *Chinese Journal of Plant Ecology* 2011;**35**:1202–8. https://doi.org/10.3724/sp.j.1258.2011.01202

Chen Y, Xu J, Gao F *et al*. Advance on the chemical and pharmacological studies on plants of *Bulbophyllum* genus. *Wuhan Zhiwuxwe Yanjiu* 2005;**3**:601–5.

Chong J, Soufan O, Li C *et al*. MetaboAnalyst 4.0: towards more transparent and integrative metabolomics analysis. *Nucleic Acids Research* 2018;**46**:W486–94. https://doi.org/10.1093/nar/gky310

Christensen DE. Fly pollination in the Orchidaceae. In: Arditti J (ed.), *Orchid Biology: Reviews and Perspectives VI*. New York, NY, US: John Wiley & Sons, 1994, 415–54.

Cuénoud P, Savolainen V, Chatrou LW *et al*. Molecular phylogenetics of Caryophyllales based on nuclear 18S rDNA and plastid *rbcL*, *atpB*, and *matK* DNA sequences. *American Journal of Botany* 2002;**89**:132–44. https://doi.org/10.3732/ajb.89.1.132

Davies KL, Stpiczyńska M. The anatomical basis of floral food-reward production in Orchidaceae. In: Teixeira da Silva JA (ed.), *Floriculture, Ornamental and Plant Biotechnology*. UK: Global Science Books, 2008, 392–407.

Davies KL, Stpiczyńska M. Labellar anatomy and secretion in *Bulbophyllum* Thouars (Orchidaceae: Bulbophyllinae) sect. *Racemosae* Benth. & Hook.f. *Annals of Botany* 2014;**114**:889–911. https://doi.org/10.1093/aob/mcu153

Delle-Vedove R, Schatz B, Dufay M. Understanding intraspecific variation of floral scent in light of evolutionary ecology. *Annals of Botany* 2017;**120**:1–20. https://doi.org/10.1093/aob/mcx055

Dressler RL. *The Orchids—Natural History and Classification*. London: Harvard University Press, 1990.

Dressler RL. *Phylogeny and Classification of the Orchid Family*. Cambridge: Cambridge University Press, 1993.

Esau K. *Plant Anatomy*. *2nd edn*. NY: John Wiley & Sons, Inc., 1965.

Farré-Armengol G, Filella I, Llusia J *et al*. Floral volatile organic compounds: between attraction and deterrence of visitors under global change. *Perspectives in Plant Ecology, Evolution and Systematics* 2013;**15**:56–67. https://doi.org/10.1016/j.ppees.2012.12.002

Fisher DB. Protein staining of ribboned epon sections for light microscopy. *Histochemie* 1968;**16**:92–6. https://doi.org/10.1007/BF00306214

Gahan PB. *Plant Histochemistry and Cytochemistry: An Introduction*. London: Academic Press, 1984.

Garay LA, Hamer F, Siegerist ES. The genus *Cirrhopetalum* and the genera of the *Bulbophyllum* alliance. *Nordic Journal of Botany* 1994;**14**:609–46. https://doi.org/10.1111/j.1756-1051.1994.tb01080.x

Gravendeel B, Smithson A, Slik FJW *et al*. Epiphytism and pollinator specialization: drivers for orchid diversity? *Philosophical Transactions of the Royal Society of London, Series B: Biological Sciences* 2004;**359**:1523–35. https://doi.org/10.1098/rstb.2004.1529

Hoang DT, Chernomor O, Von Haeseler A *et al*. UFBoot2: improving the ultrafast bootstrap approximation. *Molecular Biology and Evolution* 2018;**35**:518–22. https://doi.org/10.1093/molbev/msx281

Hu A-Q, Gale SW, Liu Z-J *et al*. Molecular phylogenetics and floral evolution of the *Cirrhopetalum* alliance (*Bulbophyllum*, Orchidaceae): evolutionary transitions and phylogenetic signal variation. *Molecular Phylogenetics and Evolution* 2020;**143**:106689. https://doi.org/10.1016/j.ympev.2019.106689

Humeau L, Micheneau C, Jacquemyn H *et al*. Sapromyophily in the native orchid, *Bulbophyllum variegatum*, on Réunion (Mascarene Archipelago, Indian Ocean). *Journal of Tropical Ecology* 2011;**27**:591–9. https://doi.org/10.1017/s0266467411000411

IOSPE (Internet Orchid Species Photo Encyclopedia). www.orchidspecies.com/indexbulb.htm (Retrieved April 21 2022).

Jaworski CC, Geslin B, Zakardjian M *et al*. Long-term experimental drought alters floral scent and pollinator visits in a Mediterranean plant community despite overall limited impacts on plant phenotype and reproduction. *Journal of Ecology* 2022;**110**:2628–48. https://doi.org/10.1111/1365-2745.13974

Jensen WA. *Botanical Histochemistry: Principle and Practice*. San Francisco, CA, USA: W.H. Freeman, 1962.

Jongejan P. Specializations in ways of attracting insects for pollination in the genus *Bulbophyllum*. In: *Proceedings of the 14th World Orchid Congress, Glasgow*, pp. 383–8, HMSO, Edinburgh, 1994.

Kaiser RAJ. *The Scent of Orchids: Olfactory and Chemical Investigations*. Netherlands: Elsevier Science Publishers B.V. Amsterdam, 1993, 264.

Kalyaanamoorthy S, Minh BQ, Wong TKF *et al*. ModelFinder: fast model selection for accurate phylogenetic estimates. *Nature Methods* 2017;**14**:587–9. https://doi.org/10.1038/nmeth.4285

Katte T, Tan KH, Su ZH *et al*. Floral fragrances in two closely related fruit fly orchids, *Bulbophyllum hortorum* and *B. macranthoides* (Orchidaceae): assortments of phenylbutanoids to attract tephritid fruit fly males. *Applied Entomology and Zoology* 2020;**55**:55–64. https://doi.org/10.1007/s13355-019-00653-x

Kindt R, Coe R. *Tree Diversity Analysis. A Manual and Software for Common Statistical Methods for Ecological and Biodiversity Studies*. Nairobi: World Agroforestry Centre (ICRAF), 2005. ISBN 92-9059-179-X.

Kirk PW. Neutral red as a lipid fluorochrome. *Stain Technology* 1970;**45**:1–4. https://doi.org/10.3109/10520297009063373

Knerr JN. The genus *Bulbophyllum*: a living fantasy. *American Orchid Society Bulletin* 1981;**50**:1051–6.

Koehler DJ, Davenport D. Ultraviolet mimicry by *Bulbophyllum lepidum*? *American Orchid Society Bulletin* 1983;**52**:359–63.

Kowalkowska AK, Kozieradzka-Kiszkurno M, Turzyński S. Morphological, histological and ultrastructural features of osmophores and nectary of *Bulbophyllum wendlandianum* (Kraenzl.) Dammer (*B.* section *Cirrhopetalum* Lindl., Bulbophyllinae Schltr., Orchidaceae). *Plant Systematics and Evolution* 2015;**301**:609–22. https://doi.org/10.1007/s00606-014-1100-2

Kowalkowska AK, Turzyński S, Kozieradzka-Kiszkurno M *et al.* Floral structure of two species of *Bulbophyllum* section *Cirrhopetalum* Lindl: *B. weberi* Ames and *B. cumingii* (Lindl.) Rchb.f. (Bulbophyllinae Schltr., Orchidaceae). *Protoplasma* 2017;**254**:1431–49. https://doi.org/10.1007/s00709-016-1034-3

Kumar S, Stecher G, Tamura K. MEGA7: Molecular Evolutionary Genetics Analysis version 7.0 for bigger datasets. *Molecular Biology and Evolution* 2016;**33**:1870–4. https://doi.org/10.1093/molbev/msw054

Majumder PL, Basak M. Cirrhopetalin, a phenanthrene derivative from *Cirrhopetalum andersonii*. *Phytochemistry* 1990;**29**:1002–4. https://doi.org/10.1016/0031-9422(90)80070-w

Majumder PL, Basak M. Two bibenzyl derivatives from the orchid *Cirrhopetalum andersonii*. *Phytochemistry* 1991a;**30**:321–4. https://doi.org/10.1016/0031-9422(91)84146-j

Majumder PL, Basak M. Two stilbenoids from the orchid *Cirrhopetalum andersonii*. *Phytochemistry* 1991b;**30**:321–4. https://doi.org/10.1016/0031-9422(91)84146-j

Mant J, Peakall R, Schiestl FP. Does selection on floral odor promote differentiation among populations and species of the sexually deceptive orchid genus *Ophrys*? *Evolution* 2005;**59**:1449–63.

Minh BQ, Schmidt HA, Chernomor O *et al.* IQ-TREE 2: New models and efficient methods for phylogenetic inference in the genomic era. *Molecular Biology and Evolution* 2020;**37**:1530–4. https://doi.org/10.1093/molbev/msaa015

Nakahira M, Ono H, Wee SL *et al.* Floral synomone diversification of *Bulbophyllum* sibling species (Orchidaceae) in attracting fruit fly pollinators. *Biochemical Systematics and Ecology* 2018;**81**:86–95.

Nunes CEP, Gerlach G, Bandeira KDO *et al.* Two orchids, one scent? Floral volatiles of *Catasetum cernuum* and *Gongora bufonia* suggest convergent evolution to a unique pollination niche. *Flora* 2017b;**232**:207–16.

Nunes ELP, Maldonado PE, Smidt EC *et al.* Floral micromorphology and anatomy and its systematic application to Neotropical *Bulbophyllum* section *Micranthae* (Orchidaceae). *Botanical Journal of the Linnean Society* 2017a;**183**:294–315.

Nunes ELP, Smidt EC, Stützel T *et al.* What do floral anatomy and micromorphology tell us about Neotropical *Bulbophyllum* section *Didactyle* (Orchidaceae: Bulbophyllinae)? *Botanical Journal of the Linnean Society* 2014;**175**:438–52. https://doi.org/10.1111/boj.12176

Nunes ELP, Smidt EC, Stützel T *et al.* Comparative floral micromorphology and anatomy of species of *Bulbophyllum* section *Napelli* (Orchidaceae), a Neotropical section widely distributed in forest habitats. *Botanical Journal of the Linnean Society* 2015;**177**:378–94. https://doi.org/10.1111/boj.12253

Oksanen J, Guillaume Blanchet F, Kindt R *et al.* Vegan: Community Ecology Package. R Package Version 2.0-8. 2013. https://cran.r-project.org/src/contrib/Archive/vegan/ Accessed 12 May 2024.

Ong PT. The pollination of *Bulbophyllum patens*. *The Orchid Review* 2011;**119**:146–9.

Ong PT. Notes on the pollination of *Bulbophyllum mandibulare* Rchb.f. *Malayan Orchid Review* 2012;**46**:67–8.

Ong PT, Hee AKW, Wee SL *et al.* The attraction of flowers of *Bulbophyllum* (Section *Sestochilus*) to *Bactrocera* fruit flies (Diptera: Tephritidae). *Malesian Orchid Journal* 2011;**8**:93–102.

Ong PT, Tan KH. Fly pollination in four Malaysian species of *Bulbophyllum* (*Section Sestochilus*) – *B. lasianthum*, *B. lobbii*, *B. subumbellatum* and *B. virescens*. *Malesian Orchid Journal* 2011;**8**:103–10.

Ong PT, Tan KH. Three species of *Bulbophyllum* Section *Racemosae* pollinated by *Drosophila* flies. *Malesian Orchid Journal* 2012;**9**:45–50.

Pang H, Datta D, Zhao H. Pathway analysis using random forests with bivariate node-split for survival outcomes. *Bioinformatics* 2020;**26**:250–8. https://doi.org/10.1093/bioinformatics/btp640

Pansarin ER, Pansarin LM. Reproductive biology of *Trichocentrum pumilum*: an orchid pollinated by oil-collecting bees. *Plant Biology* 2011;**13**:576–81. https://doi.org/10.1111/j.1438-8677.2010.00420.x

Pohl F. Zwei *Bulbophyllum*-Arten mit besonders bemerkenswert gebauten Gleit- und Klemfallenblumen. *Beihefte zum Botanischen Centralblatt* 1935;**53**:501–18.

Powers JM, Seco R, Faiola CL *et al.* Floral scent composition and fine-scale timing in two moth-pollinated Hawaiian *Schiedea* (Caryophyllaceae). *Frontiers in Plant Science* 2020;**11**:1116. https://doi.org/10.3389/fpls.2020.01116

Pridgeon AM, Cribb PJ, Chase MW *et al. Genera Orchidacearum Volume 6; Epidendroideae (Part 3)*. Oxford, UK: Oxford University Press, 2014, 4–51.

Ruzin SE. *Plant Microtechnique and Microscopy*. New York, NY, USA: Oxford University Press, 1999.

Silva UF, Borba EL, Semir J *et al.* A simple solid injection device for the analyses of *Bulbophyllum* (Orchidaceae) volatiles. *Phytochemistry* 1999;**50**:31–4.

Sirangelo TM, Rogers HJ, Spadafora ND. Multi-omic approaches to investigate molecular mechanisms in peach post-harvest ripening. *Agriculture* 2022;**12**:553. https://doi.org/10.3390/agriculture12040553

Spadafora ND, Amaro AL, Pereira MJ *et al.* Multi-trait analysis of post-harvest storage in rocket salad (*Diplotaxis tenuifolia*) links sensorial, volatile and nutritional data. *Food Chemistry* 2016;**211**:114–23. https://doi.org/10.1016/j.foodchem.2016.04.107

Stern WL, Curry KJ, Whitten WM. Staining fragrance glands in orchid flowers. *Bulletin of the Torrey Botanical Club* 1986;**113**:288–97. https://doi.org/10.2307/2996368

Stökl J, Schlüter PM, Stuessy TF *et al.* Speciation in sexually deceptive orchids: pollinator-driven selection maintains discrete odour phenotypes in hybridizing species. *Biological Journal of the Linnean Society* 2009;**98**:439–51. https://doi.org/10.1111/j.1095-8312.2009.01279.x

Stpiczyńska M, Davies KL. Evidence for the dual role of floral secretory cells in *Bulbophyllum*. *Acta Biologica Cracoviensia s. Botanica* 2016;**58**:57–69. https://doi.org/10.1515/abcsb-2016-0013

Stpiczyńska M, Davies KL, Kamińska M. Diverse labellar secretions in African *Bulbophyllum* (Orchidaceae: Bulbophyllinae) sections *Ptiloglossum*, *Oreonastes* and *Megaclinium*. *Botanical Journal of the Linnean Society* 2015;**179**:266–87. https://doi.org/10.1111/boj.12315

Stpiczyńska M, Davies KL, Zych M *et al.* Labellar secretory structures and pollinator food-rewards in representatives of Old World *Bulbophyllum* Thouars. *Flora* 2018a;**240**:98–115. https://doi.org/10.1016/j.flora.2018.01.010

Stpiczyńska M, Płachno BJ, Davies KL. Nectar and oleiferous trichomes as floral attractants in *Bulbophyllum saltatorium* Lindl. (Orchidaceae). *Protoplasma* 2018b;**255**:565–74. https://doi.org/10.1007/s00709-017-1170-4

Tan KH, Nishida R. Mutual reproductive benefits between a wild orchid, *Bulbophyllum patens*, and *Bactrocera* fruit flies via a floral synomone. *Journal of Chemical Ecology* 2000;**26**:533–46.

Tan KH, Nishida R. Synomone or kairomone? *Bulbophyllum apterum* flower releases raspberry ketone to attract *Bactrocera* fruit flies during pollination. *Journal of Chemical Ecology* 2005;**31**:509–19.

Tan KH, Nishida R, Toong YC. Floral synomone of a wild orchid, *Bulbophyllum cheiri*, lures *Bactrocera* fruit flies for

pollination. *Journal of Chemical Ecology* 2002;**28**:1161–72. https://doi.org/10.1023/a:1016277500007

Trifinopoulos J, Nguyen L-T, von Haeseler A *et al*. W-IQ-TREE: a fast online phylogenetic tool for maximum likelihood analysis. *Nucleic Acids Research* 2016;**44**:W232–5. https://doi.org/10.1093/nar/gkw256

van der Cingel NA. *An Atlas of Orchid Pollination – America, Africa, Asia and Australia*. Rotterdam, Netherlands: A.A. Balkema, 2001.

van der Pijl L, Dodson CH. *Orchid Flowers: Their Pollination and Evolution*. Coral Gables, FL, USA: University of Miami Press, 1969.

Vermeulen JJ. *Bulbophyllum*. Chapter 3. In Cribb PJ (ed.), *Orchids of Borneo*. **Vol. 2**. Kota Kinabalu: Bentham-Moxton Trust, Royal Botanic Gardens, Kew and Tuihaan Company Sdn. Bhd., 1991.

Vermeulen J, O'Byrne P. *Bulbophyllum of Sulawesi*. Kota Kinabalu: Natural History Publications (Borneo) Sdn. Bhd., 2011, 55–8.

Vermeulen, J, O'Byrne P, Lamb A. *Bulbophyllum of Borneo*. Kota Kinabalu: Natural History Publications (Borneo) Sdn. Bhd., 2015, 69–77.

Vermeulen JJ, Schuiteman A, de Vogel EF. Nomenclatural changes in *Bulbophyllum* (Orchidaceae; Epidendroideae). *Phytotaxa* 2014;**166**:101–13. https://doi.org/10.11646/phytotaxa.166.2.1

Vogel S. *The Role of Scent Glands in Pollination: On the Structure and Function of Osmophores*. Washington, D.C., USA: Smithsonian Institution, 1990.

Vogel S. Flickering bodies in floral attraction by movement. *Beiträge zur Biologie der Pflanzen* 2001;**72**:89–154.

Wang JY, Liu ZJ, Wu XY *et al*. *Bulbophyllum lipingtaoi*, a new orchid species from China: evidence from morphological and DNA analyses. *Phytotaxa* 2017;**295**:218–26. https://doi.org/10.11646/phytotaxa.295.3.2

WCSP. 2022. *World Checklist of Selected Plant Families*. Kew: Facilitated by the Royal Botanic Gardens. Published on the Internet. http://wcsp.science.kew.org/ Accessed 7 April 2022.

White TJ, Bruns TD, Lee S, *et al*. Amplification and direct sequencing of fungal ribosomal RNA genes for phylogenetics. In: Innis MA *et al*. (eds.), *PCR Protocols, A Guide to Methods and Applications*. San Diego, CA, USA: Academic Press, 1990, 315–22.

Wiśniewska N, Kowalkowska AK, Kozieradska-Kiszkurno M *et al*. Floral features of two species of *Bulbophyllum* section *Lepidorhiza* Schltr: *B. levanae* Ames and *B. nymphopolitanum* Kraenzl. (Bulbophyllinae Schltr., Orchidaceae). *Protoplasma* 2018;**255**:485–99.

Wiśniewska N, Lipińska M, Gołębiowski M *et al*. Labellar structure of *Bulbophyllum echinolabium* JJ.Sm. (section *Lepidorhiza* Schltr., Bulbophyllinae Schltr., Orchidaceae Juss.). *Protoplasma* 2019;**256**:1185–203.